

# Devonian of the Mackenzie

P. Kabanov<sup>1\*</sup>

---

*Kabanov, P., 2022. Devonian of the Mackenzie; in Sedimentary basins of northern Canada: contributions to a 1000 Ma geological journey and insight on resource potential, (ed.) D. Lavoie and K. Dewing; Geological Survey of Canada, Bulletin 609, p. 129–158. <https://doi.org/10.4095/326094>*

---

**Abstract:** This paper reviews the Devonian–Lower Mississippian strata of NTS areas 106 and 96 lying within Geo-mapping for Energy and Minerals (GEM) Mackenzie project area and its vicinity. These strata are usually well in excess of 1 km in non-eroded sections, cropping out extensively in the Cordillera and occurring in the subsurface of adjacent Interior Plains. Major tectonostratigraphic assemblages are the latest Silurian–Eifelian platform carbonates and evaporites, the latest Eifelian–Frasnian basinal mudrocks with isolated carbonate banks bundled in the Horn River Group (HRG), and the thick coarsening-upward siliciclastic succession of Frasnian–Tournaisian age deposited in the distal setting of the Ellesmerian foreland basin. A major total petroleum system of the HRG defines the economic prospectivity of Devonian strata. Review of the lithostratigraphic nomenclature is supplemented with highlights on HRG depositional environments, patterns of thermal maturity, disconformities, and sedimentary cycles in platform carbonates.

**Résumé :** Le présent article examine les strates du Dévonien-Mississippien inférieur des régions cartographiques 106 et 96 du SNRC situées dans la zone d'étude du projet Mackenzie du programme Géocartographie de l'énergie et des minéraux (GEM) et les environs. Ces strates présentent une épaisseur généralement bien supérieure à 1 km dans les coupes non érodées, affleurent largement dans la Cordillère et s'étendent dans le sous-sol des Plaines intérieures adjacentes. Les principaux assemblages tectonostratigraphiques sont constitués de roches carbonatées et évaporitiques de plate-forme du Silurien terminal à l'Eifélien; de mudrocks de bassin avec des bancs carbonatés isolés de l'Eifélien terminal au Frasnien, regroupés dans le Groupe de Horn River (GHR); et de l'épaisse succession silicoclastique à granocroissance ascendante du Frasnien au Tournaisien déposée dans le milieu distal du bassin d'avant-pays ellesmérien. La prospectivité économique des strates du Dévonien est liée à un important système pétrolier total du GHR. L'examen de la nomenclature lithostratigraphique est complété par une série de points saillants ayant trait aux milieux de dépôt du GHR, aux configurations de maturité thermique, aux disconformités et aux cycles sédimentaires dans les roches carbonatées de plate-forme.

---

<sup>1</sup>Geological Survey of Canada, 3303–33rd Street N.W., Calgary, Alberta T2L 2A7

\*Corresponding author: P. Kabanov (email: [pavel.kabanov@nrcan-mcan.gc.ca](mailto:pavel.kabanov@nrcan-mcan.gc.ca))

## INTRODUCTION

This paper presents a review of the Devonian–Mississippian strata of National Topographic System (NTS) map areas 106 and 96 lying within the Mackenzie project area of the Geo-mapping for Energy and Minerals (GEM) program and its vicinity (Fig. 1, 2). Also reviewed are the subsurface of the western Peel Plateau and adjacent outcrop belt of the eastern Richardson Mountains within NTS 106-E, -L, -M, as well as the Anderson Plain to the south of latitude 68°N (Fig. 1). The Keele Arch, or more precisely Keele tectonic zone (MacLean et al., 2015), limits the study area in the east at approximately longitude 124°W and in the south at latitude 64.5°N. This exclusion of the eastern and southern-most quadrants of NTS 96 reflects the lack of new data from these areas on which to base updates to the already existing knowledge framework (Morrow, 1991, 2012, 2018; Meijer Drees, 1993; Pugh, 1993). The Backbone Ranges region of the Mackenzie Mountains and the Wernecke Mountains is not reviewed for the same reason.

This study, commenced in 2012 at the Geological Survey of Canada (GSC), was continued during the second phase of GEM (2014–2020) as part of the Devonian Stratigraphic Framework research associated with the Shield to Selwyn Geo-transect activity of the Mackenzie project. The study builds upon extensive results from previous bedrock mapping and subsurface exploration campaigns conducted in the area by industry and national and territorial geological surveys. Major contributions to the geological knowledge of this area were made during and immediately following the Canol Pipeline project (Hume and Link, 1945; Hume, 1954), and bedrock mapping and associated research undertaken during Operation Porcupine (1962–1964; Norris, 1985), Operation Norman (1968–1970; Fallas et al., 2015), and the GEM program (2008–2013 and 2014–2020; Lavoie, Dewing et al., this volume). A major total petroleum system (TPS), with thick and geographically extensive source rocks, imparts special status to Devonian strata of this region. Conventional fields include one giant mature oilfield at Norman Wells and the recently launched oil, gas, and condensate field of Summit Creek (Hannigan et al., 2011). Research on the Devonian rocks and its TPS has advanced significantly over the last two decades through the Peel Petroleum Project undertaken by the Northwest Territories Geoscience Office and Yukon Geological Survey (2005–2009; Pyle and Jones, 2009) and the Mackenzie Plain Petroleum Project of the Northwest Territories Geological Survey (2009–2014; Pyle et al., 2014). Materials from exploration wells drilled recently by MGM Energy Corp., Husky Energy Inc., ConocoPhillips, and Shell in the central Mackenzie Valley were also used in this study. This exploration activity from 2011 to 2014 targeted the Canol shale play, a proxy name for shale hydrocarbons locked in Middle–Upper Devonian source

rocks of the Horn River Group (Hayes, 2011; Indigenous and Northern Affairs Canada, 2014; Hogg, 2015; National Energy Board – Northwest Territories Geological Survey, 2015). Economically significant mineralization is absent in the Devonian rocks of the study area but occurs farther west and south in the Mackenzie and Selwyn mountains (Dewing et al., 2006; Ootes et al., 2013).

## Tectonic and paleogeographic setting

The Lower–Middle Devonian carbonate and evaporite succession of the Delorme Group and the Arnica, Landry, Bear Rock, and Fort Norman formations (Fig. 2, 3) comprises the upper part of the lower Paleozoic–Eifelian Peel platform (also known as the Peel shelf, Mackenzie or Mackenzie–Peel platform; Norris, 1997; Morrow, 2012, 2018; Fallas et al., 2021). The Peel platform is characterized as a passive-margin succession of strata deposited in the tectonically quiet setting following Neoproterozoic–early Cambrian rifting (Cecile et al., 1997; MacLean 2011; Fallas et al., 2021). The overlying Horn River Group is latest Eifelian to Frasnian in age (Fig. 2) and corresponds to the starved basin phase characterized by a stratified water column. Although it may be envisioned as the initial phase of an accelerated subsidence in the Ellesmerian foreland basin, the spread of anoxic waters that put a halt on benthic carbonate production was likely controlled to a greater extent by a changing redox state in the adjacent Panthalassa than by genuine drowning (Kabanov, 2019; Kabanov and Jiang, 2020), as discussed below. Younger Devonian and early Tournaisian deposition of the Imperial and Tuttle formations proceeded in the distal foreland setting with accelerated clastic influx (Lane, 2007; Hadlari et al., 2009a, b). Associated syndepositional deformations are known along the eastern margin of the Mackenzie Delta, marginally occurring in the northwestern corner of the study area (Fig. 1b; Lane, 2007).

The Keele tectonic zone and Norman Wells high are two tectonic elements that likely influenced Early Devonian sedimentation (Fig. 1). The Keele Arch is an inverted-graben structure that experienced protracted evolution with subsidence and uplift events separated by phases of tectonic quiescence and peneplanation (MacLean et al., 2015). The Norman Wells high is a broad and low structure, which manifests itself as a reduction in the thickness of the Bear Rock and Fort Norman successions to less than 200 m (Fig. 3b) and a similar reduction of the underlying Delorme strata to a few metres before pinching out in the central zone of the high (Pugh, 1983; Morrow, 1991, 2018). The Keele tectonic zone has exerted a minor influence on Devonian sedimentation (Morrow, 2018), except probably for the late Silurian–earliest Devonian, when it may have remained uplifted and been the source of lithoclastic material to the sandy Tsetso Formation in the northern Root Basin (Williams, 1989; Pugh, 1993; Morrow, 2018).

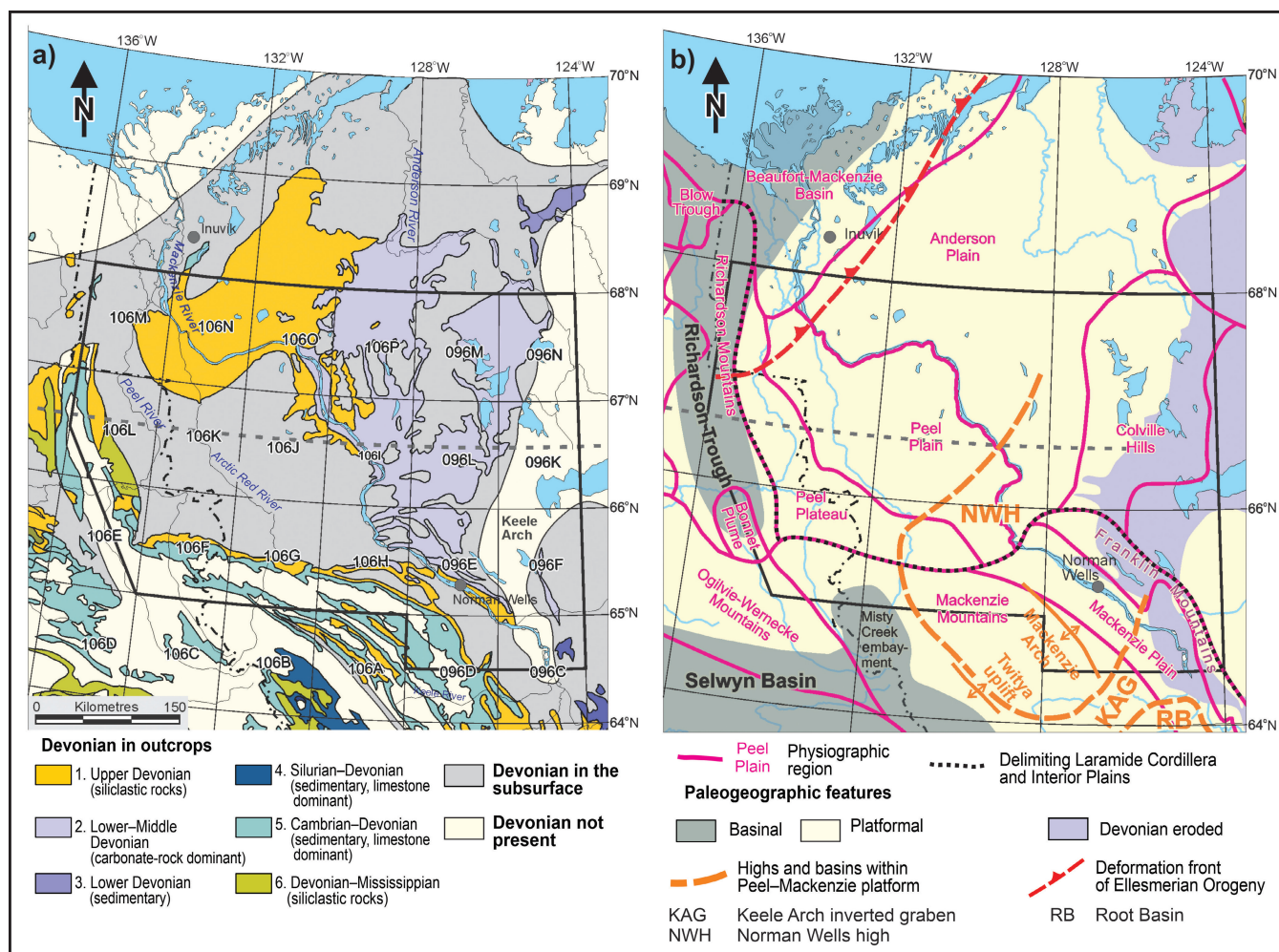


**Figure 1.** Geological and physiographic features of the study area (bold outline). **a)** Distribution of Devonian strata (faults not included) and NTS map areas partly or completely included in this study (*modified from Morrow, 2018, Fig. 1*). **b)** Physiographic regions and late Silurian–Early Devonian paleogeographic features (*adapted from Morrow, 2018, Fig. 2, 10*). Maps in Lambert conical projection.

## OVERVIEW OF DEVONIAN STRATIGRAPHY

### Sub-Devonian unconformity

An unconformity between the Ordovician–Silurian and Lower Devonian strata has been recognized based on biostratigraphic data, indicating the absence of the upper Silurian (Aitken et al., 1982) and confirmed by its fit to the North America-wide, and probably global, sea-level lowstand between the Tippecanoe and Kaskaskia supersequences of L.L. Sloss (Sloss, 1963; Morrow and Geldsetzer, 1988; Morrow, 1999, 2018). The sub-Devonian contact is concordant across the study area (Morrow, 1991, 1999; MacLean, 2012). A major truncation of pre-Devonian strata occurs immediately east and south in the Keele Arch (Cook, 1975; MacLean et al., 2015). The angular unconformity has also been documented in the proximity of the study area in

the Twitya uplift in the Backbone Ranges of the Mackenzie Mountains (Morrow, 1991). However, in areas where the Mount Kindle–Delorme contact is concordant, the evidence for a sedimentation break is rather poor, allowing for alternative interpretations. Pugh (1983, 1993) argued in favour of its conformable or largely conformable nature and recognized a more significant unconformity between his newly defined Peel and Tatsieta formations, which did not withstand further scrutiny (Morrow, 1999; Gal and Pyle, 2009). Williams (1996) concluded that the gamma-ray and sonic log markers indicated an unconformity based on the variable thickness of the Mount Kindle Formation in well sections and the sharp lithological change in cutting samples observed across the contact. However, major lithological change does not necessarily indicate a disconformable surface (Schlager, 2005), whereas disconformities separating similar lithological units are not evident in the subsurface unless thick pedogenic mantles, incised valleys, or other seismic-scale erosional forms are present (Kabanov, 2017a).



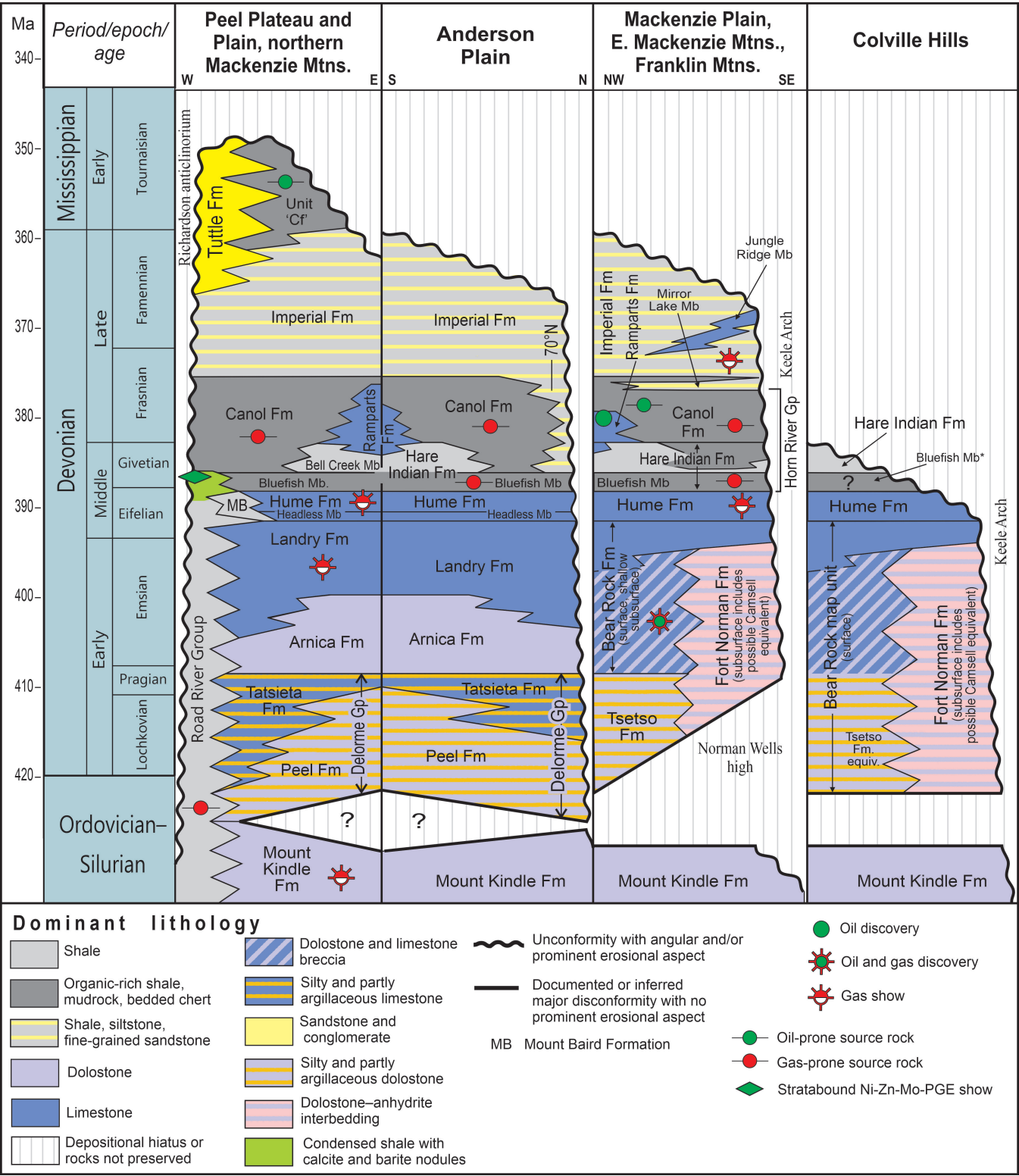


**Figure 2.** Table of Devonian formations in the study area. Stage boundaries and time scale *after* Becker et al. (2012) and Cohen et al. (2013). The Ordovician–Silurian is not time scaled. The occurrence of the Bluefish Member (\*) in the Colville Hills is inferred but not confirmed due to poor exposure (K.M. Fallas, pers. comm., 2019).



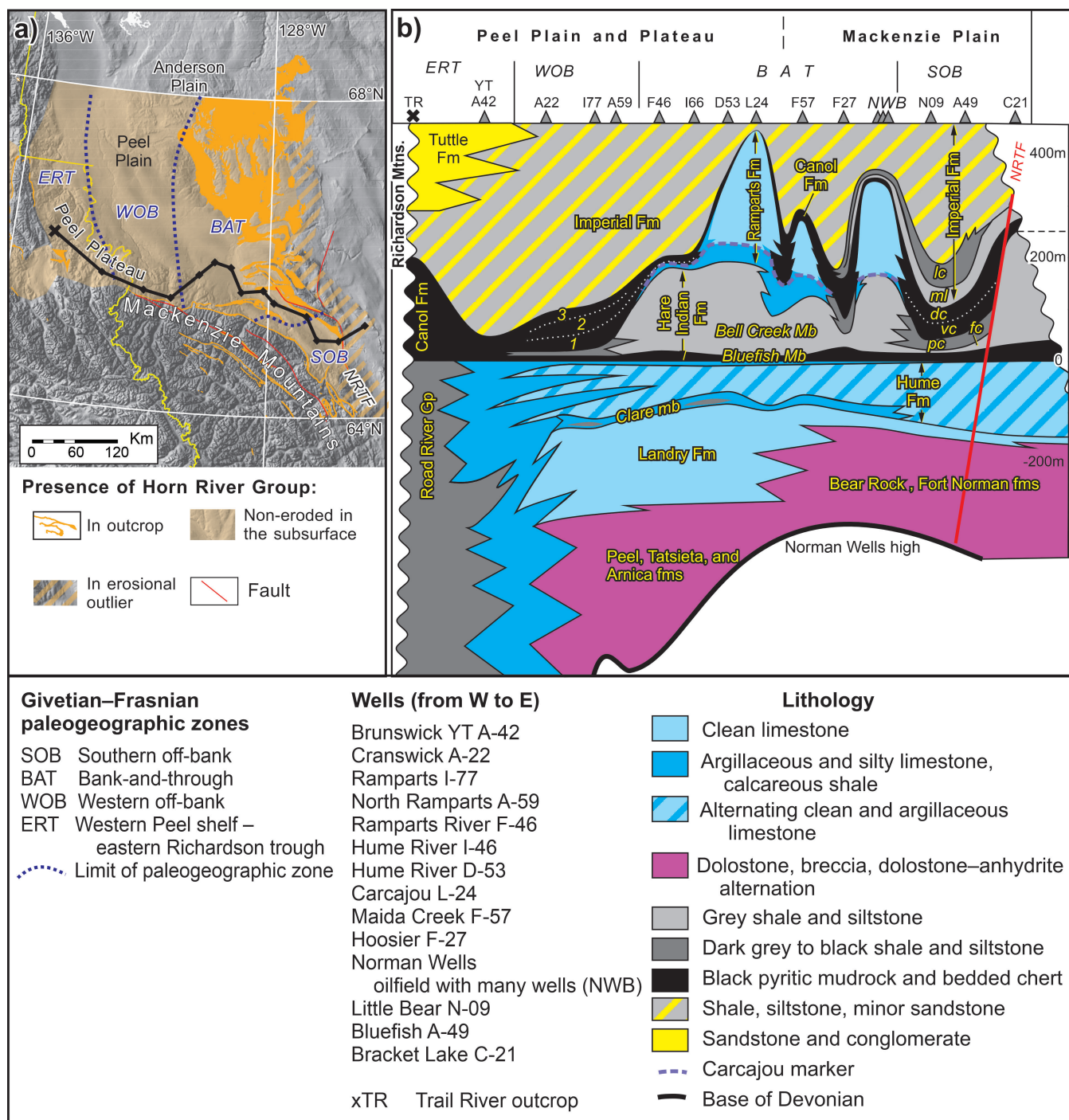


**Figure 3.** Devonian cross-section with details of the Horn River Group (*modified from Kabanov, 2017a, b, 2019*). **a)** Geographic spread of the Horn River Group between latitudes 64°N and 68°N showing the paleogeographic zones. **b)** Devonian cross-section from (a), with top of Hume Formation as zero datum, and Tuttle and Imperial formations truncated at the top; the SOB zone includes the Francis Creek (fc), Prohibition Creek (pc), Vermilion Creek (vc), Dodo Canyon (dc), Mirror Lake (ml), and Loon Creek (lc) members; the Norman Range thrust fault (NRTF) is the only tectonic element shown.

Kabanov et al. (2016b) described this contact on the unnamed ridge above Rumbly Creek (lat. 65.3725°N, long. 131.4180°W) and in the Powell Creek canyon (lat. 65.2706°N, long. 128.7798°W). Despite being typical of dolostone mediocre preservation of sedimentary and early diagenetic fabrics, fine breccias with pedogenic signatures were identified in both sections in a thin zone, probably not exceeding 1 m, just below the top of the Mount Kindle Formation. In the Powell Creek section, vadose solution breccia may have extended to a depth of approximately 10 to 12 m, based on ‘ghost’ breccia fabrics in the underlying dolostone. Morrow (1991, 1999) reported breccia and karst-like solution features penetrating down from the top of the Mount Kindle in 4 out of 20 stratigraphic sections measured through the Mount Kindle–Delorme contact. However, no evidence of early diagenetic dissolution was reported from most sections, including the Mount Kindle type locality (Table 1; Norford and Macqueen, 1975), and the richly fossiliferous facies just below the top of the Mount Kindle Formation do not show an obvious shallowing-upward progression of facies (Morrow, 1991, 1999; Pope and Leslie, 2013). Red beds near this contact are absent in the study area, except for a very thin (2–3 cm) reddish zone described at the base of the Peel dolostone at one locality (Gal and Pyle, 2009).

Quest for a major unconformity is further complicated by increasing awareness of multiple stratigraphic unconformities, some with thick clayey paleosols and underlain by many metres of karstified limestone, developed in the Lower Devonian peritidal strata and best documented in continuously cored sections (Kabanov, 2014, 2015, 2017a; Kabanov and Borrero Gomez, 2019). The paleosol features, which are interpretable at the top of the Mount Kindle Formation, are not indicative of more advanced pre-Delorme karstification and pedogenesis than those imprinted in thick intra-Devonian subaerial exposure profiles, nor do the basal Delorme strata preserve conglomerates within the study area that would indicate transgressive regolith erosion. The possible late Silurian age of the basal Delorme (Morrow, 1991; Gal and Pyle, 2009) seems to narrow the hiatus between the Mount Kindle Formation and Delorme Group, subject to further scrutiny based on new conodont data, although shallow-water facies below and above the sub-Devonian unconformity do not lend themselves particularly well to age identification. In view of the above, further statements on the nature of this surface in the study area are pending until new evidence becomes available.

## Delorme Group

The Delorme Formation was defined in the southern Mackenzie Mountains (Table 1) and subsequently elevated to group status with further subdivision into several formations, of which the Tsetso and Camsell are recognized in parts of the study area (Morrow, 1991, 2018). In the northern Mackenzie Mountains, yellow-weathered dolostone considered homotaxial with the Delorme Group was mapped as

‘unit SD’ (Aitken et al., 1982). Pugh (1983) introduced the name ‘Peel Formation’ for the pale buff dolostone overlying the Mount Kindle dolostone in the subsurface, with the type section identified in the Peel YT F-37 well (Table 1). Pugh (1983) also proposed the name ‘Tatsieta’ for the thin, partly sandy limestone with greenish shale interbeds overlying the Peel Formation and previously traced by Tassonyi (1969) as the lower limestone member of the now obsolete Gossage Formation. Continuous cores recovered from the Tenlen Lake A-73 well provide one of the best subsurface sections of the Peel–Tatsieta interval (Mackenzie, 1974). Morrow (1999) argued that the Peel–Tatsieta contact is a conformity and represents a diagenetic transition between dolostone and limestone within a single stratigraphic unit, which must be included in the Delorme Group. In the study area, both the Peel and the Tatsieta show peritidal facies assemblages, including tidal-flat laminites with buckled lamination, rip-up breccias, teepee structures, and stromatolites in the shallow-water end, and shallow-subtidal poorly fossiliferous facies in the deeper water end. In the Tatsieta limestone, the latter are represented by lime mudstones, aggregate-grain and peloidal grainstones containing small brachiopods, gastropods, and *Amphipora* (Mackenzie, 1974; Morrow, 1991, 1999; Gal and Pyle, 2009; Kabanov et al., 2016b).

In the type area of the Delorme Group and Tsetso Formation (Table 1), the Tsetso is composed of sandy dolostone, dolomitic sandstone, and greenish grey and red-mottled dolomitic–argillaceous rocks unconformably onlapping the Ordovician–Silurian carbonate rocks (Morrow, 1991; Meijer Drees, 1993). The Tsetso Formation intergrades with, and is overlain by, the evaporitic Camsell Formation. In outcrops, the latter is composed of solution-collapse breccia of crystalline limestone, probably dedolomite, submerged in a coarsely crystalline calcite–limonite matrix (Morrow, 1991; Meijer Drees, 1993). In the subsurface, it is composed of alternating bedded anhydrite and dolostone (Meijer Drees, 1993). The Delorme strata are thin on the periphery of the Norman Wells high and wedge out in its central area (Pugh, 1983, 1993; Morrow, 1991). Thin Delorme strata are considered unmappable in outcrops eastward of longitude 129.4°W (Fallas and MacNaughton, 2021a). In the broad peripheral area of Norman Wells high, it is difficult to assert the presence or absence of Delorme strata in the subsurface, as they cannot be separated from the Fort Norman Formation in coreless boreholes (Meijer Drees, 1993; Pugh, 1993). Thin, nonbrecciated dolostone between the top of the Mount Kindle and the base of the typical Bear Rock breccia is frequently observed in the eastern Mackenzie Mountains, extending into the peripheral zone of the Norman Wells high (K.M. Fallas, pers. comm., 2019); for example, this dolostone is 53 m thick in the Powell Creek canyon (Kabanov et al., 2016b). The lower 22 m of the dolostone preserves buckled lamination, ‘bird’s eye’ fenestrae, and minor stromatolites characteristic of the Peel Formation, whereas the upper 31 m is more massive, partly fossiliferous, and may correlate with the Tatsieta–lower Arnica formations (Kabanov et al., 2016b).

**Table 1.** Alphabetical compilation of type and reference sections of Silurian–Devonian lithostratigraphic units in the study area.

Lithostratigraphic unit	Author	Type section	Latitude	Longitude	Reference section in study area	Latitude	Longitude
Arnica Fm	Douglas and Norris, 1961	South side of First Canyon of S. Nahanni River (Douglas and Norris, 1977)	61.283	–124.233	Northern Mackenzie Mtns. section LG-B (Gal et al., 2009)	65.503	–132.795
Bear Rock Fm	Hume and Link, 1945	Bear Rock Cliff, Mackenzie River 3.5 km N of the mouth of Great Bear River (Morrow and Meijer Drees, 1981)	64.912	–125.683			
Bell Creek Mb of Hare Indian Fm	Pyle and Gal, 2016	Mountain River, NE Mackenzie Mtns. (Pyle and Gal, 2016)	65.239	–128.594			
Bluefish Mb of Hare Indian Fm	Pugh, 1983	Bluefish Creek/River, tributary of Hare Indian R. (NTS 106-I); R.J. Kirker cited in Tassonyi (1969)	n.a.	n.a.	Powell Creek (Pugh, 1983; Pyle and Gal, 2016; Kabanov et al., 2016c)	65.277	–128.7890
Camsell Fm	Douglas and Norris, 1961	Whittaker and Delorme Ranges, NTS 95-K, S. Mackenzie Mtns.; no type section designated	n.a.	n.a.			
Canol Fm	Bassett, 1961	Powell Creek, NE Mackenzie Mountains (Bassett, 1961; Braun, 1966; Kabanov et al., 2016c)	65.277	–128.774			
Canyon Mb of Imperial Fm	Hume, 1954	Cores at 373–404 m of Canyon Creek no. 1 (G-51) well (Tassonyi, 1969); revisited by Kabanov et al. (2016a)	65.173	–126.416	Canyon Mb type B: cored section at 1904.9–1910.4 m of Mirror Lake N-20 (Kabanov and Gouwy, 2017)	64.998	–126.8026
Carcajou Mb of Ramparts Fm	Carcajou marker; Tassonyi, 1969	Carcajou Ridge; measured by D.J. McLaren in 1961 (Fig. 5 in Tassonyi, 1969)	65.633	–128.252			
Delorme Gp	Delorme Fm (Douglas and Norris, 1961)	Pastel Creek on Delorme Range, S. Mackenzie Mtns. (Douglas and Norris, 1961; Morrow and Cook, 1987)	62.792	–125.267			
Dodo Canyon Mb of Canol Fm	Kabanov and Gouwy, 2017	Dodo Canyon East outcrop, E. Mackenzie Mtns. (Pyle and Gal, 2012; Pyle et al., 2014)	65.0078	–127.3249			
Fort Norman Fm	Meijer Drees, 1993	411.4–679.7 m of Willow Lake L-59 well; no cores were cut	62.1372	–121.9333	Vermilion Ridge No. 1 (N-28) well (Tassonyi, 1969); 315.5–563.0 m (Hogue and Gal, 2008); 10% is cored	65.131	–126.0851
Francis Creek Mb of Hare Indian Fm	Kabanov and Gouwy, 2017	Francis Creek, Norman Range of Franklin Mtns. (Kabanov et al., 2016a)	65.2419	–126.3875			
Hare Indian Fm	Kindle and Bosworth, 1921	Mouth of Hare Indian River downstream of Fort Good Hope (Kindle and Bosworth, 1921)	66.2900	–128.6000	Mountain River tributary, NE Mackenzie Mtns. (Gal et al., 2009)	65.239	–128.5945
Headless Fm	Douglas and Norris, 1961	Meilleur Creek and the First Canyon on S. Nahanni River at Headless Range, S. Mackenzie Mtns. (Douglas and Norris, 1961); Ram Plateau, S. Mackenzie Mtns. (Morrow and Cook, 1987)	61.7500	–124.4167	Headless Mb: cored section at 1276.8–1293.6 m of Clare F-79 well (Kabanov and Borrero Gomez, 2019; Kabanov and Deblonde, 2019)	67.139	–133.2412
Horn River Gp	Whittaker, 1922	Horn River, E. Great Slave Plain; promoted to group by Williams (1983) and Pugh (1983)	61.733	117.750	Mountain River tributary, NE Mackenzie Mtns. (Pyle and Gal, 2016)	65.239	–128.5949



Table 1. (cont.)

Lithostratigraphic unit	Author	Type section	Latitude	Longitude	Reference section in study area	Latitude	Longitude
Hume Fm	Bassett, 1961	Hume River, N. Mackenzie Mtns. (Bassett, 1961)	65.3357	-129.9687			
Imperial Fm	Hume and Link, 1945; redefined by Bassett, 1961	Imperial River at the front of Mackenzie Mtns. (Hume and Link, 1945; Bassett, 1961)	65.1138	-127.8608			
Jungle Ridge Mb of Imperial Fm	Hume and Link, 1945	493–543 m of Bluefish no. 1A (A-37) well (C.R. Stelek in Hume and Link, 1945; Tassonyi, 1969)	64.9355	-125.8494			
Kee Scarp Mb of Ramparts Fm	Kee Scarp Mb (Jones and Gal, 2007) = Reef member of Tassonyi (1969)	Kee Scarp Ridge, Norman Range, 9.3 km NE of Norman Wells (Gal et al., 2009)	65.2800	-126.7600			
Landry Fm	Douglas and Norris, 1961	Delorme Range, S. Mackenzie Mtns.; no type section designated	n.a.	n.a.	Cored section at 949.1–1301.5 m, Kugluk N-02 well (Kabanov, 2013, 2014, 2015)	68.5320	-131.5245
Loon Creek Mb of Imperial Fm	Kabanov and Gouwy, 2017	Cored section at 1653.25–1625.2 m of Loon Creek O-06 well (Kabanov et al., 2016a)	65.0977	-127.0104			
Mirror Lake Mb of Imperial Fm	Kabanov and Gouwy, 2017	Cored section at 1965.4–1942.0 m of Mirror Lake N-20 well (Kabanov et al., 2016a)	64.9980	-126.8026			
Mount Baird Fm	Norris, 1985	Outcrop at tributary of Snake River, NTS 106-F, northwestern Mackenzie Mtns.	65.4528	-133.5833			
Mount Kindle Fm	Williams, 1922	NE face of Mount Kindle, S. Franklin Mtns. (Norford and Macqueen, 1975)	63.3491	-123.1975			
Peel Fm	Pugh, 1983	Peel R. YT F-37 well (Pugh, 1983); 2983.1–3327.2 m (Fraser and Hogue, 2007); no cores	66.9394	-134.8656	Cored section of Tenlen Lake A-73 well (Mackenzie, 1974)	67.8688	-130.7250
Prohibition Creek Mb of Hare Indian Fm	Kabanov and Gouwy, 2017	Prohibition Creek, Norman Range of Franklin Mtns. (Kabanov et al., 2016a)	65.1881	-126.2137			
Ramparts Fm	Kindle and Bosworth, 1921	Ramparts Gorge, Mackenzie R. near Fort Good Hope (Kindle and Bosworth, 1921)	66.2308	-128.7212			
Road River Gp	Jackson and Lenz, 1962	Tetlit Creek, tributary to Road River, E. Richardson Mtns. (Jackson and Lenz, 1962)	66.73	135.77			
Tatsieta Fm	Pugh, 1983	994–1055 m of Grandview Hills no. 1 (A-47) well (Tassonyi, 1969; Pugh, 1983); no cores were cut	67.1033	-130.8772	Cored section of Tenlen Lake A-73 well (Mackenzie, 1974)	67.8688	-130.7250
Tsetso Fm	Meijer Drees, 1993	750.4–1202.7 m of Ochre River I-15 well, Great Slave Plain (Meijer Drees, 1993)	63.4126	-122.7841			
Tuttle Fm	Pugh, 1983	Peel R. YT F-37 well, 980–1021 m (Pugh, 1983); 215.8–966.2 m (Dixon, 2012)	66.9394	-134.8656			
Vermilion Creek Mb of Canol Fm	Kabanov and Gouwy, 2017	Vermilion Creek, Norman Range of Franklin Mtns. (Pyle and Gal, 2013)	65.1431	-126.0440			

Co-ordinates (NAD 83, UTM 8–11U, degree decimals) are given for borehole surfaces (referenced to the Kelly bushing) or bases of units in outcrops, where this detail is available in a cited source, and are shaded in pink if they occur outside the study area. Obsolete formations (e.g. Gossage, Cranswick, Prongs Creek) are not included.

## Arnica, Landry, Bear Rock, and Fort Norman formations

These four divisions bundle Lower and lower Middle Devonian carbonate and anhydrite units contacting each other through lateral facies and diagenetic transitions and partly occurring in stratigraphic succession (Fig. 2). The Arnica, Landry, Bear Rock, and Fort Norman formations are routinely traced in well sections (Pugh, 1983, 1993; Hogue and Gal, 2008). These four units appear as one horizon on legacy high-resolution seismic-reflection lines, where the Devonian carbonate succession is thick (e.g. transect A1 in MacLean, 2012). Quite often, the Delorme–Hume carbonate units cannot be confidently subdivided using legacy-quality seismic-reflection data (MacLean, 2012).

### Arnica Formation

The Arnica Formation consists mostly of dolostone; the stratotype is located in the southern Mackenzie Mountains, and the reference section designated in the study area (Table 1). The Arnica is mapped in the northern Mackenzie Mountains to the west of longitude 129.4°W and north of latitude 64°N (Morrow, 1991; Fallas and MacNaughton, 2021a, b) and is recognized on airborne survey images by its stripy dark and pale appearance (Morrow, 1991, 1999; Gal et al., 2009; Kabanov et al., 2016b). The alternation of dark and pale colours matches fairly well the cyclic changes in facies. The darker bands reveal shallow-subtidal carbonate rocks with copious *Amphipora*, and the paler bands tend to preserve traces of laminar intertidal facies (Morrow, 1991; Gal et al., 2009). Dolostone units in the Arnica succession are usually coarsely crystalline, sucrosic, and fabric destructive, but incomplete dolomitization preserves intervals of variously dolomitized limestone. Several homogeneously grey intervals 10 to 50 m thick reveal shallow to deep subtidal facies of fossiliferous lime mudstone and wackestone (Kabanov et al., 2016b). These ‘sea-level highstand intervals’ are also found in the continuously cored section of the Kugaluk N-02 well (Kabanov, 2015). Subaerial-exposure profiles with vadose solution cavities, breccias, and pedogenic claystones are detectable in the upper parts of Arnica cycles in outcrops and cores, where dolomitization did not completely destroy these features (Kabanov, 2015; Kabanov et al., 2016b).

### Landry Formation

The Landry Formation type section is in the southern Mackenzie Mountains (Table 1). Pugh (1993) proposed to recognize the local reference section in the Grandview Hills no. 1 (A-47) well, which has only 18% of core coverage. The continuously cored section of the Kugaluk N-02 well, although more distant from the outcrops of the northern Mackenzie Mountains, may serve as a better reference section (Kabanov, 2014, 2015). In the study area, the Landry Formation consists of

light to dark grey and brownish, well-bedded limestone showing pronounced metre-scale peritidal cyclicity with numerous subaerial exposure surfaces (Morrow, 1991; Kabanov, 2014, 2015). The lower contact was described as conformable (Gal and Pyle, 2009) or diagenetic (Kabanov, 2014), denoting in the latter case the limestone–dolostone transition that varies in appearance from a sharp, of metre scale, to a thick, up to 140 m, alternation of limestone and dolostone (Kabanov, 2015). Eastward of longitude 129.4°W, the Landry Formation is considered unmappable (Fallas and MacNaughton, 2021a) but is recognized in many sections as the Landry Member of the Bear Rock Formation, a thin-bedded (~20–100 m) unit of variously argillaceous and partly bituminous dolostone and limestone retaining features of the characteristic peritidal cyclicity of the Landry Formation (Morrow, 1991). Brecciation in the Landry Member is significant and normally increases downward, marking its gradation to the Bear Rock breccia (Morrow, 1991; Kabanov et al., 2016b).

### Bear Rock Formation

The name ‘Bear Rock’ experienced a long transformation in meaning and usage since the original definition (Table 1). Milestone reviews of the Bear Rock Formation were given by Bassett (1961), Aitken et al. (1982), Morrow (1991), Meijer Drees (1993), Gal et al. (2009), and Gouwy et al. (2017). The Bear Rock Formation, in its type facies, pertains to chaotic collapse breccia of dolostone and limestone occurring in outcrops and in the shallow subsurface. This breccia originated from dissolution of evaporite interbeds in the Fort Norman Formation (Fig. 2; Morrow and Meijer Drees, 1981; Morrow, 1991, 2018; Meijer Drees, 1993). Typical Bear Rock breccia consists of a mosaic of packbreccias with cemented and open interfragment space intergrading with particulate rubble floatbreccias (Morrow, 1982, 1991). Size of fragments typically ranges between sand-grain size and approximately 1 m (Morrow, 1991), with reports of tabular blocks nearing 10 m in length (Kabanov et al., 2016b). Gal et al. (2009) proposed to abandon formation status for the Bear Rock and recognized instead the Bear Rock breccia facies within the Fort Norman Formation. However, the Bear Rock Formation retains its practical application in the study area (Fig. 2) as a bedrock map unit bundling typical Bear Rock breccia and less or nonbrecciated carbonate strata between the top of the Mount Kindle and the base of the Hume formations (Gouwy et al., 2017). The Bear Rock is mapped in the study area to the east of longitude 129.4°W in the eastern Mackenzie Mountains, Franklin Mountains, Great Slave Plain, Anderson Plain, and Colville Hills (Fallas, 2013a, b, 2018a–d; Fallas and MacNaughton, 2013, 2021a, b; Fallas et al., 2013). In the Colville Hills and adjacent northern Great Bear Plain, the Bear Rock map unit brackets strata recognizable as belonging to the Delorme Group and Arnica and Landry formations that are overall less affected by solution brecciation than the Bear Rock type facies (Cook and MacLean, 1993; Gouwy et al., 2017).

## ***Fort Norman Formation***

‘Fort Norman’ is the name proposed by Meijer Drees (1993) to formalize Tassonyi’s (1969) evaporitic member of the Bear Rock Formation (Table 1). The formation is composed of laminar, finely crystalline and nodular anhydrite, and similarly laminar dolostone, with horizons of breccia and rip-up clasts (Meijer Drees, 1993). Anhydrite prevails in most localities, whereas dolostone becomes more important in the upper Fort Norman in several wells (Pugh, 1993). Predominantly subsurface occurrence of the Fort Norman Formation is complemented with rare outcrops, where sulphate bands are sufficiently preserved (Gal et al., 2009). Meijer Drees (1993) noted the cyclic character of the Fort Norman, with metre-scale sedimentary sequences composed of dolostone–anhydrite couplets. The Fort Norman is absent in the Keele Arch (Meijer Drees, 1993) but reappears farther south in the Root Basin, where the thickness of undivided Fort Norman and Camsell evaporites exceeds 1500 m (Morrow, 1991; Pugh, 1993). In the Root Basin, the Camsell and Fort Norman formations are separated by the normal-marine bedded carbonate unit some 130 to 170 m thick known as the ‘Arnica platform dolomite’ (Williams, 1975). In the central Mackenzie Valley, the Fort Norman Formation ranges between 200 and 400 m in thickness (Pugh, 1993; Hogue and Gal, 2008) and is depicted as directly onlapping the disconformable contact at the top of the Mount Kindle Formation. It is possible that this succession includes the thin, unrecognized equivalent of the Delorme Group and Camsell Formation in its basal part (Fig. 2; Meijer Drees, 1993; Pugh, 1993; Hogue and Gal, 2008).

## ***Hume Formation***

The Hume Formation is a succession of medium-bedded, variously argillaceous, locally dolomitic limestones and calcareous shales (Bassett, 1961). The Hume has stratotype located in the study area (Table 1) and shows a consistent thickness between 60 and 140 m across most of the area (Kabanov and Deblonde, 2019). Thicker Hume sections occur in the southwestern corner of the study area (up to 180 m), where the Hume grades into the upper Road River Group, and in the Keele tectonic zone of the Mackenzie Plain, where it reaches 224 m in the Summit Creek K-44 well. The Hume is dominated by bioturbated subtidal carbonate-platform facies with rich assemblages of benthic fossils (Pugh, 1983, 1993; Norris, 1985; Morrow, 1991). Internal subdivisions of the Hume Formation were based on strongly and weakly alternating argillaceous intervals. Five informal members (three limestones and two intervening calcareous shales to limestones) have been traced by Tassonyi (1969) and Pugh (1983) in the subsurface of the study area. Later, Pugh (1993) concluded that the upper shaly unit could not be traced widely and proposed a threefold subdivision with the lower, prominently argillaceous and thin-bedded unit named the ‘Headless Member’, after its apparent formation-rank equivalent in the southern Mackenzie Mountains and the subsurface of the Great Slave Plain (Law, 1971; Morrow,

1991; Meijer Drees, 1993). In outcrops, the twofold subdivision into a lower, more argillaceous and recessive member and upper, somewhat cleaner and more resistant limestone member was found most reliable (Morrow, 1991; Gal et al., 2009). In cores from the central Mackenzie Valley and in adjacent Norman Range outcrops, the upper, less argillaceous part of the Hume is different from the type section at Hume River and more northerly sections (e.g., Clare F-79 well; Kabanov and Borrero Gomez, 2019). The upper Hume there is thicker bedded and dominated by massive sparsely fossiliferous lime mudstone and wackestone with local bird’s-eye fenestrae (e.g., Kabanov et al., 2019). However, very shallow-water tidal-flat laminities are thin and rare even in these sections, and discontinuities of potential subaerial origin are likely rare and poorly developed, with no known reports of distinct paleokarsts or paleosols. Absence of these most obvious signatures of shallowing impedes recognition of metre-scale sea-level cycles. Gal et al. (2009) recognized ‘cleaning-up’ cycles of more argillaceous and less argillaceous limestones 2 to 10 m thick within the Hume Formation, but no supporting evidence of shallowing-upward progression of facies was given. The signs of sea-level change are most pronounced in the basal ‘Headless’ unit, as discussed below, which is generally consistent with interpretation of the Hume as representing a single cycle or sequence (Morrow, 1991, 2018).

## ***Base of the Hume Formation***

The Landry–Hume contact was originally characterized as “sharp and probably disconformable”, except for “some localities with a thin transitional zone” (Bassett, 1961, p. 487). Subsequent examinations have confirmed the conformable and gradational nature of the basal part of the Hume Formation as it appears on well logs and in cored sections (Pugh, 1983, 1993; Kabanov, 2014). Gal et al. (2009) admitted the conformable nature of the Landry–Hume contact but pinpointed it at a sharp contact of limestone and thin dark grey shale in some outcrops. Perception of the base of the Hume as a disconformity historically changed to that of a conformity with recognition of the presence of a transitional unit between the Bear Rock breccia and the argillaceous base of the Hume Formation (Landry Member of Bear Rock Formation; Morrow, 1991). Transition from the clean limestone of the uppermost Landry Formation to the argillaceous limestone and shale of the basal Hume Formation is usually distinct on gamma-ray, sonic, and resistivity logs, and in seismic transects it matches with a ‘top of the Landry’ seismic-reflection marker (MacLean, 2012).

## ***Drowning unconformity at the top of the Hume Formation***

The top of the Hume Formation is a prime well-log and seismic marker (Pugh, 1993; MacLean, 2012) interpreted as a conformity, a paraconformity, or an erosional



surface imprinting a sedimentary hiatus (Gal et al., 2009). The nature of the Hume Formation top deserves additional scrutiny, since this hiatus reappears in recent versions of the table of formations (Rocheleau and Fiess, 2014; Morrow, 2018). In outcrops, the top of the Hume is table flat, unless tectonically displaced (Kabanov and Gouwy, 2017), but southward of the study area, the correlated surface in the top of the Lonely Bay and Nahanni formations is locally outgrown by Givetian carbonate pinnacles referred to as ‘Horn Plateau reefs’ (Vopni and Lerbekmo, 1972; Meijer Drees, 1993; Corlett and Jones, 2011). Carbonate pinnacles of similar age are unknown in the study area, but the Trail River H-37 well in the region of paleogeographic transition from the Hume carbonate platform to the Richardson trough basin reveals an unusual 131 m section of clean benthic carbonate underlain by typical argillaceous–carbonate facies of the Road River Group. This clean carbonate is overlain by the abnormally thin Canol Formation of only 5.8 m in thickness (Kabanov and Deblonde, 2019). The Trail River H-37 well section is unique in the study area, probably because of the sparse coverage of exploration drilling but, when considered at a larger geographic scale, it finds its counterpart in the Parker River J-72 well of northeastern Banks Island, in Northwest Territories (Kabanov, 2018). In the Parker River J-72 well, the carbonate rocks below the atypically thin basinal mudrock are biostratigraphically dated as Givetian, and short diamond core cut from the lower part of that carbonate section exhibits carbonate mud-mound fabrics with *Stromatactis* (Kabanov, 2018). Both sections are surmised to represent isolated carbonate pinnacles developed on basin-facing platform slopes similarly to, and coevally with, the Horn Plateau reefs (Kabanov and Deblonde, 2019).

Kabanov et al. (2016b) and Kabanov and Gouwy (2017) have examined the contact between the Hume Formation and Bluefish Member in three diamond cores and three outcrop sections. In two of these, hardgrounds were observed in the rugged, pyritized and chertified top, whereas the other four localities, including the type section of the Bluefish Member at Powell Creek (Table 1), showed condensed transitional intervals 0.5 to 2.6 m thick punctuated by smooth discontinuities. This transitional limestone contains brachiopod banks with *Eliorhynchus castanea* (Meek) and phosphatic inarticulate brachiopods, but no stromatoporoids or other fossils from shallow-water carbonate-platform assemblages (Kabanov and Gouwy, 2017). Tentaculitids appear in this transitional unit and become rock forming upward from the base of the Bluefish Member. The top of this transitional unit is usually smooth and storm scoured. The basal few centimetres of the Bluefish Member characteristically contain imbricated brachiopod shells mixed with diverse tentaculitids, sometimes dominated by tentaculitids with rare brachiopod fragments. Bioturbation in this basal Bluefish bed drops abruptly and, right above this basal bed, declines to zero. Enrichment in aluminum-normalized U and Mo increases from moderate in the base of the Bluefish Member to a major spike of high values in an area approximately 2.0 m above the base referred to as ‘the first

anoxic horizon of the Horn River Group’ or AH-I (Kabanov, 2019). Gradational character similar to that displayed by the Hume–Bluefish contact was observed in cores from the Kugaluk N-02 well, just north of the study area (Kabanov et al., 2016d; Kabanov and Borrero Gomez, 2019). Further evidence of the absence of a hiatus at the top of the Hume is provided by conodonts, which indicate by their presence that the top of the Hume and the base of the Bluefish occur in the single *Polygnathus ensensis* Zone (Gouwy, this volume).

Given the collective evidence, the Hume–Bluefish contact is interpreted as a drowning unconformity with no evidence of a geologically appreciable hiatus (Kabanov, 2017a; Kabanov and Gouwy, 2017). Drowning unconformities are ‘maximum flooding surfaces’ specific to carbonate platforms (Schlager, 1989) caused by the demise of the carbonate-production factory through genuine drowning, burial under siliciclastic strata, or shallowing of the chemocline in the basin (Kabanov, 2017a). Drowning unconformities are within-trend drowning (‘flooding’) surfaces in sequence stratigraphy (Catuneanu, 2006) or type 3 sequence boundaries (Schlager, 2005). The sediment-starved condensed character of the lower Bluefish Member indicates that benthic carbonate production was stopped by the rise of the chemocline in clear waters rather than burial under siliciclastic rocks (Kabanov, 2019). Carbonate pinnacles outgrowing the smothered carbonate platform fit in this interpretation as loci, probably on antecedent seafloor elevations, where benthic carbonate production was able to keep the bank top aggrading above anoxic waters.

### ***The basal shaly unit of the Hume Formation***

The basal shaly unit of the Hume Formation, or the ‘Headless Member’ of Pugh (1993), is traced with confidence in the northern part of the study area and farther north in the Anderson Plain. Its physical characteristics are attested to by continuously cored sections at 930.6 to 949.1 m from the Kugaluk N-02 well, 427.0 to 440.7 m from the Crossley Lake South K-60 well (formation tops from Kabanov, 2018), 410.0 to 427.3 m from the Tenlen Lake A-73 well, and 1276.8 to 1293.6 m from the Clare F-79 well (formation tops from Kabanov and Deblonde, 2019). The Clare F-79 is a good candidate for the reference section of the basal shaly unit (Table 1) because it offers the greatest amount of rock from the 3.5 in. (8.9 cm) slabbed core available for future analyses in a continuous middle Hume–upper Landry section (Kabanov and Borrero Gomez, 2019). Three other sections are represented by thin 2 in. (5.1 cm) slabbed cores.

The character of the basal shaly unit is very similar in all studied cores. It is a dolomitic calcareous shale to argillaceous limestone (i.e. marlstone) characterized by suppressed bioturbation, with the bioturbation index dropping to 2 or 3 (Taylor and Goldring, 1993; Taylor et al., 2003), as opposed to thoroughly bioturbated limestones of the overlying Hume Formation and underlying uppermost few metres of the Landry Formation. The basal shaly unit is also characterized

by rhythmic bedding, interpreted as distal tempestites deposited during the ‘Headless highstand’ (Kabanov, 2018). In the Kugaluk N-02 well, elemental data with flat logs of aluminum-normalized Mo, V, Pb, Zn, Cu, Ni, and U indicate lack of authigenic enrichment of redox-sensitive trace metals (Kabanov, 2015). This indication of an oxic sedimentary regime can be extrapolated to most of the other sections in which black-shale units are absent. Minor black-shale occurrences within the basal shaly unit were reported from outcrops (Gal et al., 2009) and wells (Tassonyi, 1969; Pugh, 1983), including a distinct tongue of black pyritic shale in the basal part of the Hume Formation intersected by the Cranswick A-42 well (Pugh, 1983).

Subsurface traceability of the basal argillaceous unit of the Hume Formation is good across the Anderson Plain and Peel Plain and Plateau to the north of latitude 66.3°N and west of longitude 129.3°W, but to the south and east of these lines, it is frequently masked by the development of an argillaceous facies in the upper Hume with a similar log response. This is reflected in the sharply uneven thickness of the basal Hume unit on the isopach map between latitudes 66.3°N and 65.5°N. Farther south, in the subsurface of the Mackenzie Valley, this unit cannot be separated with any confidence from the overlying Hume Formation (Kabanov and Deblonde, 2019). This loss of traceability is the first reason for questioning the applicability of the name ‘Headless’ to this formation in the study area. The second reason is the uncertainty of correlation with the Headless Formation near its type area. These sections are dominated by poorly fossiliferous, peloidal–ostracodal–charophytic argillaceous limestone and dolostone containing conglomerates and breccias (Meijer Drees, 1993). The Headless Formation was correlated with the lower part of the Hume Formation in the study area based on total gamma-ray and sonic responses, by which a somewhat more argillaceous unit of variable thickness was traced between overlying and underlying cleaner carbonate strata (Meijer Drees, 1993; Pugh, 1993). This correlation was supported with sparse biostratigraphic data (Chatterton, 1978). The Headless Formation is intergrading in part with the Ebbutt Member of the evaporitic Chinchaga Formation known to contain at least one internal disconformity (Belyea, 1970). Cores from the Ebbutt D-50 and Fort Simpson M-70 wells at the Headless or Ebbutt interval reveal multiple subaerial exposure surfaces and shallow-water, maybe partly nonmarine ostracodal–charophytic facies (Kabanov and Borrero Gomez, 2019). Some subaerial surfaces exhibit thick floatbreccia and pedogenic claystones, indicating protracted development (Kabanov, 2017a; Kabanov and Borrero Gomez, 2019). This feature makes the Headless Formation disparate from the basal shaly member of the Hume in the study area, which bears evidence of uninterrupted transgression and sea-level highstand.

## Road River Group

The Road River Group is a thick (up to ~3 km) succession of black graptolitic shale, calcareous shale, chert, resedimented bioclastic limestone, lime mudstone, and conglomerates filling the Cambrian–Middle Devonian Richardson trough and the Misty Creek embayment of the Selwyn Basin (Norris, 1997; Morrow, 1999; Pyle and Gal, 2009; Strauss et al., 2020). As reviewed by Morrow (1999), the original Ordovician–Silurian age assignment of the Road River Formation (Jackson and Lenz, 1962) has been subsequently expanded to the late Cambrian through Middle Devonian. The Road River Group occurs in the study area only marginally in map areas NTS 106-L, -E, -F, where well sections reveal interfingering facies of the upper Road River Group and Hume Formation (Kabanov and Deblonde, 2019). Norris (1968) proposed the name ‘Prongs Creek’ for the Devonian part of the Road River, which he defined as strata occurring between the stratigraphically highest specimens of graptolites and the base of the Canol or Imperial formations. Later, Norris (1985, 1997) disclaimed ‘Prongs Creek’ as lacking lithological criteria for the justification of its base, whereas paleontological criteria such as the disappearance of graptolites were not considered pertinent for a lithostratigraphic subdivision (North American Commission on Stratigraphic Nomenclature, 2005). Referring to a personal communication from M.P. Cecile, Morrow (1999) published new names for the informal units of the upper Road River Group. The uppermost unit of mainly or completely Devonian age, which previously appeared on geological maps (Norris, 1981; Cecile et al., 1982), was given the name ‘Vittrekwa’, but D.W. Morrow (1999) warned against formal usage of the ‘Vittrekwa’ until adequate characterization was made publicly available. Strauss et al. (2020) upgraded the Vittrekwa unit to formal usage by assigning the type section (Table 1) and giving its lithological, carbon isotope ( $\delta^{13}\text{C}_{\text{org}}$ ), and biostratigraphic characterization, by which it was assigned to the latest Silurian to Middle Devonian. The Vittrekwa Formation is 100 to 412 m thick in the Richardson anticlinorium. It is composed of alternating black pyritic and brown calcareous shales and lime mudstones bearing graptolites in the basal part, and ostracods, tentaculitids, and locally benthic macrofossils throughout the formation (Morrow, 1999; Strauss et al., 2020). Subsurface expression of the Vittrekwa remains unexplored, except for the single Caribou N-25 well, where its base was picked at an abrupt downward increase of gamma-ray and sonic logs (Morrow, 1999). Pre-Devonian subdivisions of the Road River Group are reviewed in Morrow (1999), Pyle and Gal (2009), and Strauss et al. (2020).

## *Stratigraphy of the Peel platform margin in map area NTS 106-F*

In the northwestern Mackenzie Mountains lying within the Snake River map area (NTS 106-F), the Lower–Middle Devonian strata are transitional in their character and

thickness between the Road River basinal facies and Peel shelf carbonate units (Morrow, 1999, 2018). Norris (1968) applied the name ‘Cranswick Formation’ to open-marine fossiliferous limestone exposed in a small area within NTS 106. The Cranswick Formation of Norris (1968) was equivalent to the Arnica and Landry formations of the adjoining Peel shelf. The name ‘Mount Baird’ was introduced by Norris (1985) to bundle the package of greenish grey calcareous shale and minor argillaceous limestone varying in thickness from 326 m to less than 100 m (Morrow, 1999). The Mount Baird is an equivalent of the Hume Formation of the Peel shelf (Norris, 1985, 1997). It is overlain by the Canol Formation and separated from the Cranswick of Norris (1968) by a thin (90 m and less) tongue of black pyritic shale assigned to the Road River Group (Morrow, 1999). The Mount Baird Formation is not recognized in the subsurface (Fraser and Hogue, 2007; Hogue and Gal, 2008). The Cranswick Formation is now regarded as obsolete, and these strata are included in the Landry Formation (Morrow, 1999; Gal et al., 2009).

### ***Barite-polymetallic horizon at the top of the Road River Group***

The top of the Road River Group is characterized by the development of a thin, 1 to 4 m, concretionary zone with nodules of authigenic calcite and barite (Gadd and Peter, 2018; Gadd et al., 2020). At the top of this nodular zone, some outcrop sections show a thin (<10 cm) crust of Ni-Zn-Mo-PGE ore referred to as the hyper-enriched black shales (HEBS; Fig. 3b; Hulbert et al., 1992; Gadd and Peter, 2018). Up to three stacked HEBS horizons were found in the uppermost Road River Group in outcrops along the Peel River (Fraser et al., 2017; Gadd et al., 2020). The upper HEBS horizon is assumed to be the marker for the contact between the Road River Group and the Canol Formation. The HEBS crusts formed through metal scavenging in the seawater under a regime of extreme sediment starvation (Gadd and Peter, 2018). The Road River–Canol contact has been the subject of particularly detailed examination in the Trail River outcrop (Fraser, 2014; Hutchison and Fraser, 2015; Fraser and Hutchison, 2017). Fraser and Hutchison (2017) speculated that the thin (2.3 m), concretionary, metal-enriched zone transitional between the Road River and the Canol may have been deposited over a protracted period of time spanning the latest Eifelian to Givetian and thus be an equivalent of the entire Hare Indian Formation. Rhenium–osmium geochronology and conodont data narrow the age of the upper crust of the HEBS and the Road River–Canol contact to the latest Eifelian to early Givetian (Gadd et al., 2020).

### **Horn River Group**

The name ‘Horn River shale’ was extended to the study area from the eastern Great Slave Plain (Table 1) following a long history of redefinitions and changing usage reviewed

by Pugh (1983), Williams (1983), Pyle and Gal (2016), and Kabanov and Gouwy (2017). Tassonyi (1969) first proposed application of the name ‘Horn River Formation’ in the study area to refer to the undivided Hare Indian and Canol shales, in those locations where the Ramparts Formation was absent. The crucial step in bundling the Hare Indian, Ramparts, and Canol formations into the Horn River Group was the abandonment of a sub-Canol unconformity, with conclusive evidence discussed by Williams (1983), Pugh (1983), Muir (1988), and Kabanov and Gouwy (2017). However, a hiatus at the base of the Canol can still be encountered in recent lithostratigraphic charts (Rocheleau and Fiess, 2014; Morrow, 2018). The Horn River Group is briefly described below, following the layout of paleogeographic zonation proposed by Kabanov and Deblonde (2019).

### ***Hare Indian, Ramparts, and Canol formations***

The uppermost Eifelian–Frasnian Horn River Group occurs across a vast area in the Northwest Territories, both in the Cordillera and in the adjacent Interior Plains (Morrow, 2012, 2018), and is equivalent to the Canol Formation of northern Yukon (Fig. 3, 4). The occurrence of thick (150–400 m) Hare Indian and Ramparts strata defines the bank-and-trough (BAT) paleogeographic zone (Fig. 3, 4). This succession of fossiliferous grey shale, siltstone, and limestone conformably overlies the basal black-shale unit of the Hare Indian Formation called the ‘Bluefish Member’. The Bell Creek Member of the BAT zone is a thick (up to 190 m) succession of grey, variously calcareous shale and siltstone representing basin-filling clinoforms or ‘deltaic shale lobes’ sourced from the easterly located Laurentian landmass (Muir and Dixon, 1985; Muir, 1988).

The Ramparts Formation consists of three main parts and is best described as carbonate banks developed above thick shale lobes of the Hare Indian Formation. The lower platform (or lower ramp) member is informal and therefore not in Table 1. It refers to an argillaceous and silty fossiliferous limestone intergrading with, and overlying, the upper portion of the Bell Creek Member of the Hare Indian Formation. The middle Carcajou member (Table 1) is a thin (2–3 m, rarely up to 7 m) limestone unit containing benthic fossils. The Carcajou is distinguished from underlying and overlying Ramparts limestones by its dark argillaceous and bituminous matrix; it is also identified in many wells by its elevated gamma-ray response. Quite commonly, the base and top of the Carcajou cannot be precisely defined due to development of similar gamma-ray spikes in the lower Kee Scarp Member. In some sections at Norman Wells, the limestone of the lower platform member is not sufficiently developed, and the Carcajou marker overlies the calcareous fossiliferous siltstone of the Hare Indian Formation (Fig. 3, 4). The Kee Scarp Member (Table 1) is defined as a portion of the Ramparts Formation developed above the Carcajou marker (Fig. 4; Gal et al., 2009). The Kee Scarp forms spatially restricted carbonate banks and pinnacles and is composed of



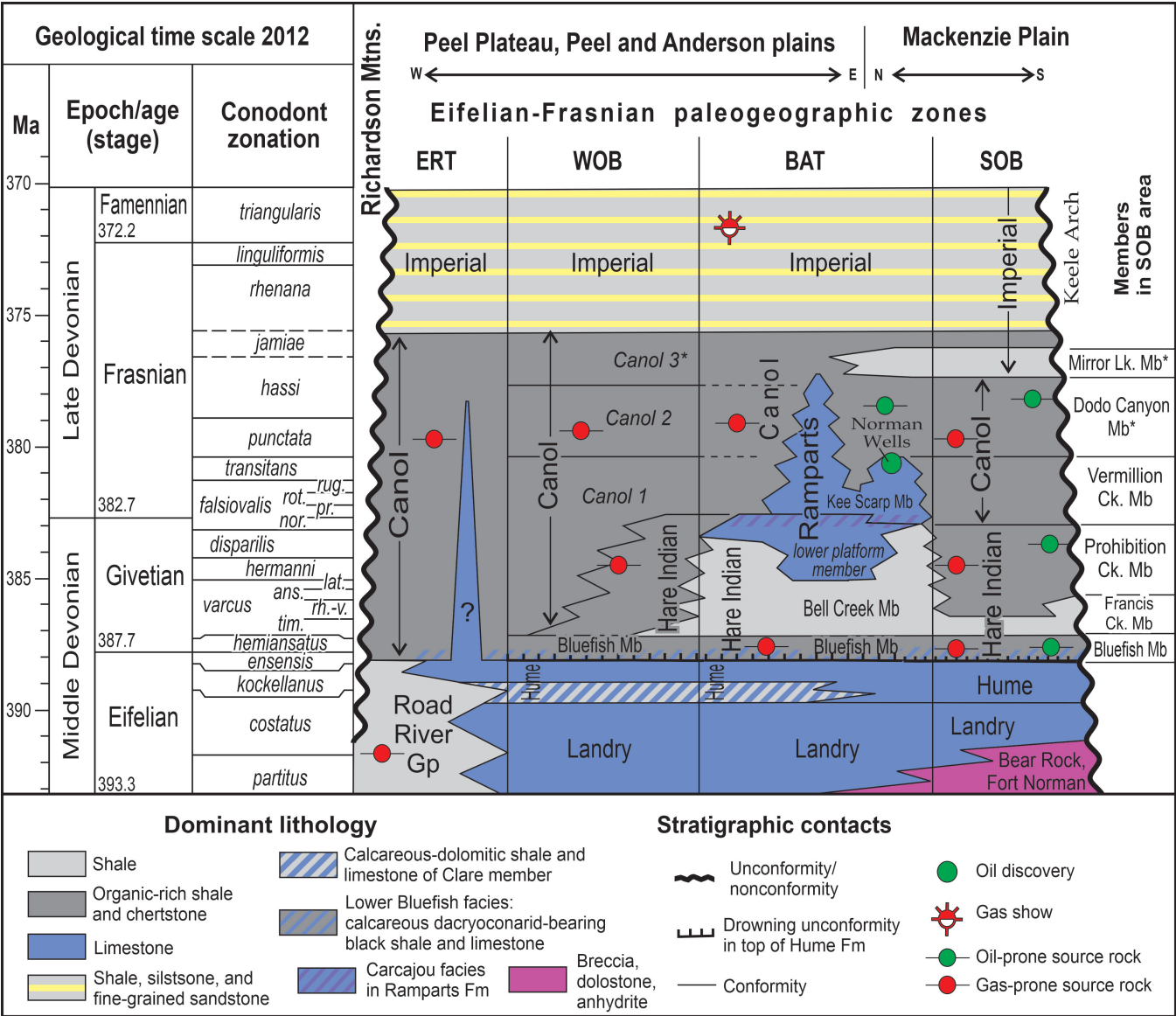


**Figure 4.** Eifelian–Frasnian chronostratigraphic chart, showing the lithostratigraphy across the study area (modified from Kabanov and Deblonde, 2019) and the eastern Richardson trough–western Peel (ERT), western off-bank (WOB), bank-and-trough (BAT), and southern off-bank (SOB) paleogeographic zones. Conodont zonation is based on summary and new data of S.A. Gouwy as reviewed in Kabanov (2019). Alternative Givetian–Frasnian conodont zones *timorensis* (*tim.*), *rhenanus-varcus* (*rh.-v.*), *ansatus* (*ans.*), *latifossatus/semialternans* (*lat.*), *norrisi* (*nor.*), *pristina* (*pr.*), *rotundiloba* (*rot.*), and *rugosa* (*rug.*) are from Narkiewicz and Bultynck (2007) and Becker et al. (2016). Asterisk (\*) denotes units with notably poor age control.

relatively clean limestone with stromatoporoids and pachy-porid tabulate corals (dominantly genus *Thamnopora*). In the best-studied examples, it reveals the backstepping, tapering-upward stacking pattern of subtidal–intertidal cycles/parasequences (Muir et al., 1984; Yose et al., 2001). Minor lithostratigraphic units historically linked to the Ramparts Formation and not included in Table 1 are the Charrue sandstone and the informal ‘allochthonous limestone member’ (Pugh, 1983). The latter refers to thin (up to 5.5 m) strata of local occurrence composed of graded laminated calcisiltites and bioclastic calcarenites partly interbedded with

Canol-type black shale. These allochthonous limestones were interpreted as off-reef debris (MacKenzie, 1970, 1973; Pugh, 1983).

The Canol Formation is the geographically extensive unit traced within the limits of the ancestral North America (east of the Tintina fault zone) from its eastern erosional edge to the western limits of the Eagle Plain, where it likely merges into the thicker McCann Hill Chert of the western Yukon and adjacent Alaska (Norris, 1997; Hutchison and Fraser, 2015). The southern limit of the Canol Formation lies

approximately at latitude 63°N, where the nomenclature of the Givetian–Frasnian black shales changes, and the northern limit has been identified around longitude 70°N, where the Canol loses its physical and log signatures and merges with the Devonian clastic wedge of the western Arctic Islands (Kabanov, 2018; Kabanov et al., 2020). Within the study area, the Canol is composed of siliceous pyritic shale and muddy chertstone containing nodules and beds of authigenic carbonate (Pyle and Gal, 2016; Fraser and Hutchison, 2017; Kabanov and Gouwy, 2017; Kabanov, 2019). The Canol is thick (>60 m in most well sections) in off-bank areas but thins to a few metres in the BAT zone (Fig. 3b, 4), and its high gamma-ray log signature disappears completely above the tallest carbonate banks intersected by wells in the subsurface of map area NTS 106-H (Tassonyi, 1969; Pugh, 1983; Kabanov and Deblonde, 2019).

Two scenarios may be invoked to explain the fact that the Canol pinches out above tall carbonate banks: 1) small banks of benthic carbonate may have survived rises of the chemocline in the Canol basin until their burial by Imperial siliciclastic rocks; 2) benthic carbonate production ceased at one of the anoxic events recognized within the upper Canol (Kabanov, 2019), but the tallest carbonate buildups remained in a sediment-bypass regime until their burial by Imperial siliciclastic rocks. The lithostratigraphic chart of the BAT zone depicts the first scenario (Fig. 4).

### ***Paleogeographic zones and refined lithostratigraphy***

Kabanov and Deblonde (2019) recognized four paleogeographic zones in the study area, each with a separate set of subformational units (Fig. 3, 4). This zonation originated during the latest Eifelian–Frasnian through widespread and uniform deposition of the Bluefish Member, followed by progradation of a deltaic complex onto the part of the study area called the ‘bank-and-trough’ paleogeographic zone (BAT; Kabanov and Gouwy, 2017). These clinoform-shaped deposits of the Hare Indian Formation formed seafloor highs above the chemocline, allowing growth of the carbonate platforms (banks) of the Ramparts Formation upon the waning of the siliciclastic influx (Muir and Dixon, 1985; Muir, 1988; Kabanov, 2019). The Ramparts is of very uneven thickness and is altogether completely missing from some sections (e.g. Hoosier F-27 well), which justifies referring to the area as a ‘bank-and-trough’ zone (Kabanov and Gouwy, 2017).

In present-day structural configuration, the BAT zone separates the black-shale basin of the Horn River Group from the ‘southern off-bank’ (SOB) zone and a broader area in the Peel Plain and Plateau straddling the ‘western off-bank’ (WOB) and the ‘western Peel–eastern Richardson trough’ (ERT) paleogeographic zones (Fig. 3). In the SOB zone, the thin black-shale succession of the upper Hare Indian Formation is subdivided into the Francis Creek and Prohibition Creek members, and that of the overlying Canol

Formation into the Vermilion Creek and Dodo Canyon members (Table 1). The Francis Creek is a thin (3–17 m), recessive, fissile, dark grey shale separating two more resistant black shales of the Bluefish and Prohibition Creek members (Kabanov et al., 2016a; Kabanov and Gouwy, 2017). Previously the Francis Creek and Prohibition Creek members were traced by Pugh (1993) as an informal black-shale member of the upper Hare Indian and by Pyle et al. (2014) as an atypical Bell Creek Member. In the Canol Formation, the Vermilion Creek Member is separated from the Dodo Canyon Member by the 15 to 20 m thick interval with the increased content of siliciclastic fines, authigenic dolomite, and drops in authigenic Mo and U (Kabanov and Gouwy, 2017). Tassonyi (1969) recognized this interval previously as a Canyon Creek electric-log marker. Formation tops and isopach maps of new subdivisions within the SOB zone can be found in Kabanov and Deblonde (2019). Kabanov and Gouwy (2017) also redefined the Bell Creek Member of Pyle et al. (2014) and Pyle and Gal (2016), restricting it to thick grey shales and siltstones typifying the upper Hare Indian Formation in the BAT zone.

Transition of the Horn River Group from the BAT to the WOB zone occurs across the 131st meridian (Fig. 3), where the Bell Creek Member thins into black-shale strata of only 10 to 26 m in thickness and the carbonate units of the Ramparts disappear altogether, whereas the Canol Formation thickens inversely to more than 60 m (Kabanov and Deblonde, 2019). Historically, the overall recessive black-shale package developed between the Hume limestone and the basal Imperial sandstone to the west of the BAT zone was mapped as the ‘undivided Dheci unit’ at the surface (Aitken et al., 1982) and the Horn River Formation in the subsurface (Pugh, 1983). The Hare Indian is traced only in the eastern WOB zone, where the low-resistivity and lowered gamma-ray marker of the upper Hare Indian can be traced. Kabanov and Deblonde (2019) recognized three informal members of the Canol Formation in the WOB zone (Fig. 3, 4). These units are traced in wells using total gamma-ray, resistivity, and sonic logs and are correlated with the outcrops at Rumbly Creek with spectral gamma-ray logs (Kabanov et al., 2016b). The Canol 2 retains signatures characteristic of the Dodo Canyon Member in the SOB zone. The Canol 1 appears to be an equivalent of the Vermilion Creek Member of the SOB zone in its main upper part. In wells of the western part of the WOB zone, where the upper Hare Indian is no longer traceable, the Bluefish Member and the basal part of Canol 1 merge into one high-radioactivity horizon with gamma-ray responses in excess of 300 API (Kabanov and Deblonde, 2019).

The Canol 3 of the WOB zone is the transitional unit between the siliceous shales and cherts of the Canol Formation and grey siliciclastic-rich shales of the basal Imperial Formation (Kabanov and Deblonde, 2019). The Canol 3 has been assigned with controversy to either the Canol as its ‘upper recessive unit’ (Pyle et al., 2014) or the Imperial Formation (Pyle and Gal, 2016). The decision to

leave Canol 3 within the Canol Formation (Kabanov and Deblonde, 2019) complies with the definition of the Canol top in the type section at the level with nodular carbonate beds in the 30 m above the base of the allochthonous limestone (Kabanov et al., 2016b). This is consistent with earlier Canol Formation top picks at Powell Creek (Braun, 1966; Lenz and Pedder, 1972).

### ***Traceability of the Canol Formation in the ERT zone augmented with ED-XRF***

In the ERT zone between longitude 134°W and the eastern erosional edge of the Richardson anticlinorium, the Canol Formation no longer retains resistivity and total gamma-ray signatures of its WOB subdivisions. Instead, many borehole sections show deceptive total gamma-ray responses of the Canol occurring partly in the background of the underlying Road River Group and the overlying shale of the Imperial Formation (Kabanov and Deblonde, 2019). Deceptively low total gamma-ray responses also characterize the upper Canol in the reference outcrop at Trail River, although lithological descriptions, gamma-ray spectrometry, and lithogeochemical proxies clearly define the Canol Formation as an integral unit different in many respects from the underlying and overlying strata (Fraser, 2014; Fraser and Hutchison, 2017).

Improvement in picking the top and base of the Canol in the subsurface of the ERT zone is achieved through X-ray fluorescence (XRF) surveying of cutting samples (Fig. 5). Measurements were made using the Bruker Tracer IV-SD analyzer on samples in their original vials covered with Prolene® 4 µm film. The instrument was set up on a customized GeoQuant Majors factory calibration of a single 15 kV excitation. This GeoQuant Majors method reports elements from Mg to Zn on control materials, but in cutting samples, it only delivers a qualitative result of the relative abundance of major oxides, where original stratigraphic signals manifest themselves with various clarity through sample contamination caused by cavings and drilling mud additives (Kabanov et al., 2020).

Major-oxide XRF measurements were obtained in eight wells through the intervals assigned to the Canol Formation in the ERT zone (Fraser and Hogue, 2007; Hogue and Gal, 2008). The Canol is characterized by lowered siliciclastic components proxied by  $\text{Al}_2\text{O}_3$  and the terrigenous input proxy (TIP), whereas  $\text{SiO}_2$  stays elevated, attesting to the cherty lithology (Fig. 5). The TIP is the sum of the major refractory oxides  $\text{Al}_2\text{O}_3$ ,  $\text{Fe}_2\text{O}_3$ ,  $\text{TiO}_2$ , and  $\text{K}_2\text{O}$  residing predominantly in siliciclastic rocks (Hildred et al., 2011; Pyle and Gal, 2016). The elements bound in siliciclastic rocks show a strong covariation with  $\text{SiO}_2$  in the Imperial Formation and weakened, sometimes nonexistent covariation in the Canol Formation (Fig. 5). In the upper Canol, co-manifesting spikes of MgO and CaO, sometimes a single spike of CaO, probably indicate the presence of authigenic carbonate rocks. The pyritic aspect of the Canol is expressed in the raised S content

and its relatively strong covariation with Fe. This feature of S–Fe logs is repeated in many sections downhole into the Road River Group, which may be the result of a mixture of signals from uphole caving chips and the Road River–Hume rocks. This S–Fe covariation is not characteristic of the Imperial Formation (Fig. 5). The base of the Canol is usually distinct on borehole logs and, in XRF logs, shows a major increase in CaO. The XRF logs appear especially useful in defining the Canol in wells that were abandoned without geophysical logging, as exemplified by the Peel River YT N-77 well (Fig. 5b).

### **Imperial and Tuttle formations**

The uppermost portion of the Paleozoic succession preserved in the Cretaceous subcrop in the study area is composed of the thick siliciclastic sequence of the Imperial and Tuttle formations (Aitken et al., 1982; Pugh, 1983, 1993; Allen et al., 2009; Dixon, 2012). The Imperial and Tuttle formations were defined within the study area (Table 1) and represent the southern extension of the Devonian clastic wedge filling the Ellesmerian foreland basin (Braman and Hills, 1992; Lane, 2007). Cumulative thickness of these strata exceeds 2500 m in the northwestern part of the study area (Pugh, 1983). The name ‘Imperial Formation’ pertains to the succession of finer grained siliciclastic rocks composed of alternating units of soft, variously fossiliferous shale, siltstone, and fine-grained sandstone (Pugh, 1983, 1993; Dixon, 2012). The Imperial Formation is traced across the study area and beyond, southward to latitude 63°N (Dixon, 2012) and northward approximately to the mainland shoreline, where the nomenclature changes to that of the units of the Devonian clastic wedge of the western Arctic Islands (Embry and Klován, 1976; Dewing and Embry, 2007; Kabanov et al., 2020). The Imperial Formation is dominated by turbiditic facies and composed of seismic-scale clinoforms having prograded from the northeast. The Imperial contains rhythmic slope-fan sand lobes and is interpreted as a shallower water unit in the Mackenzie Valley and a deeper water unit in the western part of the study area (Hadlari et al., 2009a, b).

The Tuttle Formation is a thick (874 m in the type section) sequence of sandstone, shale, and conglomerate that occurs in conformable contact and partly lateral interfingering with the Imperial Formation (Pugh, 1983; Fraser and Allen, 2007; Allen et al., 2009; Dixon, 2012). Geographic occurrence of the Tuttle in the study area is limited to the eastern flank of the Richardson anticlinorium and the western Peel Plateau (Fraser and Allen, 2007; Allen et al., 2009). Palynomorph data indicate the Tuttle succession is middle Famennian–late early Tournaisian (Braman and Hills, 1992; Allen et al., 2009).

Age populations of detrital zircons recovered from Imperial Formation sandstone indicate provenance from northwestern Laurentia, with an admixture of material from exotic sources representing a broad circum-Arctic region, the most paleogeographically remote of which could be the



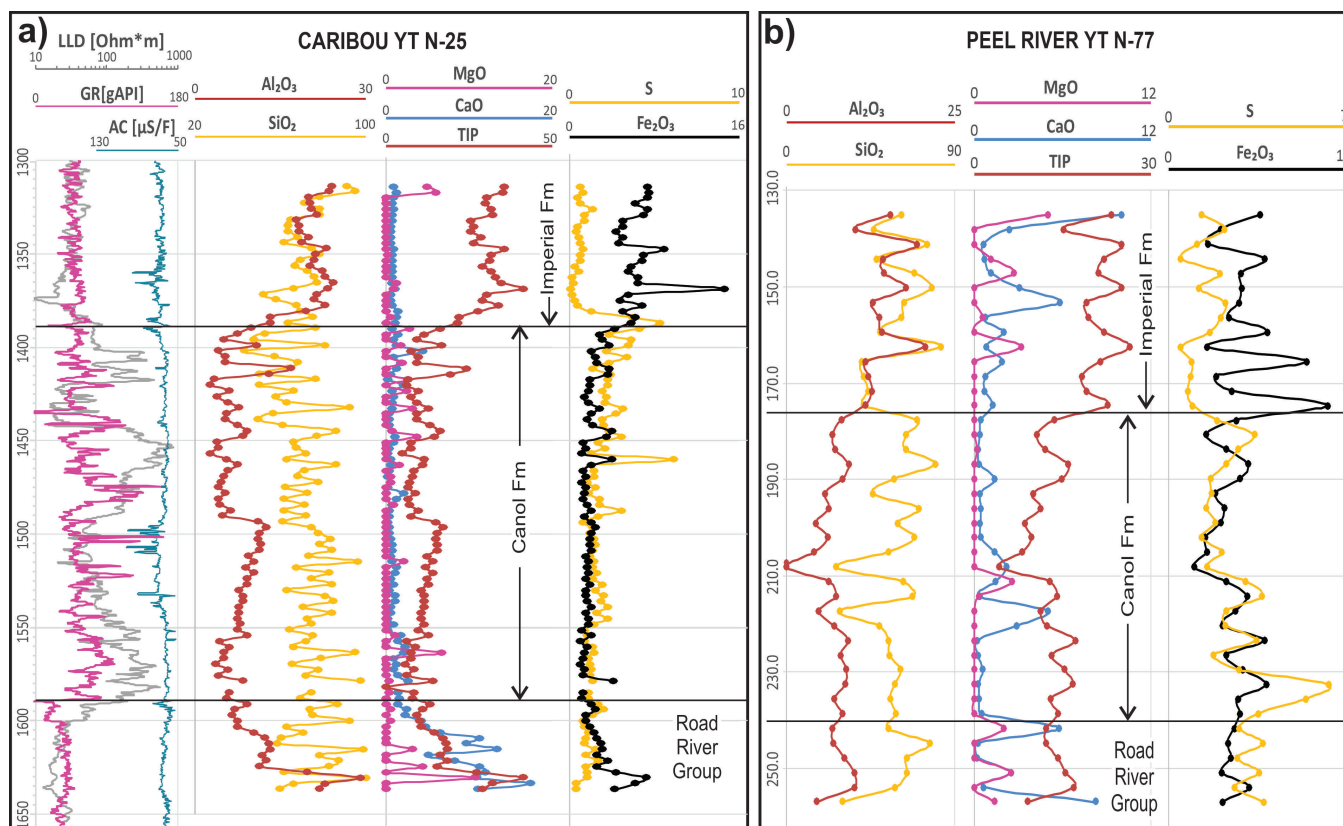


**Figure 5.** Two examples of energy dispersive-X-ray fluorescence logs through the Canol Formation in wells of the eastern Richardson trough–western Peel paleogeographic zone. *Modified from Kabanov and Deblonde (2019).* Measured depth is in metres. **a)** Caribou YT N-25 well. **b)** Peel River YT N-77 well, which has not been logged after drilling.

Baltica Craton and the Timanian orogenic belt (Beranek et al., 2010; Lemieux et al., 2011). The clastic rocks of the Tuttle Formation contain more proximal zircon age markers than those of the Imperial Formation, which suggests some restriction in provenance during the late Famennian and Tournaisian, when coarser Tuttle clastic units encroached into the study area (Lemieux et al., 2011). The following paragraphs review the subformational lithostratigraphic units recognized within the Imperial–Tuttle succession.

### *Canyon Member*

The Canyon Member, also referred to as the ‘basal Imperial sandstone’ (Hadlari et al., 2009a, b), is recognized in the subsurface of the Mackenzie Plain and adjacent outcrops, where the fact it disappears justified the historical name ‘Canyon Creek sandstone lentil’ (Tassonyi, 1969; Pugh, 1993). The typical Canyon Member (i.e. Canyon type A of Kabanov and Gouwy, 2017) is a 25 to 33 m thick sandstone-dominated unit; in some sections it is dominated by siltstone with minor or no sandstone (Tassonyi, 1969; Pugh 1983, 1993). Kabanov et al. (2016c) reviewed cores from the type section (Table 1) and two other wells in the type area used by Tassonyi (1969) in his correlations. The Canyon Member

in these localities is composed of very fine-grained quartzose sandstone, minor siltstone and shale; the stratal pattern is organized in thick sandstone-dominated Bouma rhythms and represents the coarsening-upward succession of a prograding turbidite fan (Hadlari et al., 2009b). The sandstone disappears in well sections drilled a few kilometres south-westward (paleogeographically offshore) from the type area, and the Canyon Member thins into an interval of less than 10 m, with important siltstones, but otherwise not markedly different from overlying and underlying shales. Kabanov and Gouwy (2017) referred to this interval as the ‘Canyon Member type B’ (Table 1) and showed its traceability in the subsurface with the negative total gamma-ray excursion.

### *Mirror Lake and Loon Creek members*

Historical placement of the Canyon sandstone lentil at the base of the Imperial Formation (Aitken et al., 1982) conflicted with growing awareness of a relatively thin unit of the Imperial shale separating the Canyon sandstone and the Canol Formation (Bassett, 1961; Pugh, 1993). Examination of borehole materials from recent exploration activity in the Mackenzie Valley shed clarity on the stratigraphy of the Canol–Imperial transitional interval (Kabanov

and Gouwy, 2017) and led to significant improvement in formation top picking (Kabanov et al., 2016a; Kabanov and Deblonde, 2019).

The Mirror Lake Member (Table 1), a grey fissile shale conformable and gradational at its top and base, is notably recessive in outcrops; pyritized acritarchs and similarly pyritized sponge spicules are preserved in cores, but these have usually been destroyed by weathering in outcrops. The Mirror Lake is enriched in clays (mostly illite; Kabanov et al., 2016d) and contains minor siltstone and very fine-grained sandstone. No bioturbation or benthic fossils other than sponge spicules were encountered. Occurrence of siderite makes the Mirror Lake even more distinct from the Canol, where siderite is not encountered unless the formation top is miscorrelated (Kabanov et al., 2016d). The Mirror Lake Member is traced in the subsurface to the east of longitude 128°W (NTS 96-C, -D, -F), where its thickness changes from 5–10 m on top of the Ramparts carbonate banks to 21–59 m in the SOB zone (Kabanov et al., 2016a). The thicker and lithologically distinct Mirror Lake Member produces a so-called ‘top Canol seismic reflector’ in parts of the SOB zone (Enachescu et al., 2013a). The Mirror Lake thins, grades to black shale, and loses its geophysical signature westward of longitude 128°W. In NTS 106, the Mirror Lake is no longer recognizable, probably merging into the ‘upper recessive unit’ of the Canol Formation *sensu* Pyle et al. (2014).

The overlying Loon Creek Member is composed of black siliceous mudrock in its basal half or third resembling the Canol Formation and was therefore historically assigned to the Canol in many instances (Kabanov and Deblonde, 2019). However, the basal mudrock of the Loon Creek is less pyritic than the Canol Formation and usually replete with hyalosponge spicules, which are relatively rare in the Canol (Kabanov and Gouwy, 2017; Kabanov and Jiang, 2020). The basal mudrock of the Loon Creek grades upward into dark grey silty shale and siltstone with siderite nodules and abundant sponge spicules characterizing the upper Loon Creek Member. The top of the Loon Creek is constrained by the Canyon type B gamma-ray log marker, and the upper half or even two-thirds of the Loon Creek grades laterally into coarser grained siliciclastic units of the Canyon type A (Kabanov and Gouwy, 2017).

### ***Jungle Ridge Member***

Hume and Link (1945) introduced the name ‘Jungle Ridge’ to refer to an argillaceous and silty limestone in the lower to middle Imperial Formation. The Jungle Ridge occurs in the southeastern portion of the study area, in the subsurface of the Mackenzie Plain and adjacent outcrops. In the type section, the calcareous interval assigned to the Jungle Ridge is about 60 m thick (Table 1). The Jungle Ridge limestone is traced as an interval approximately 30 to 40 m

thick in wells of the northern and central Mackenzie Valley, where it occurs in a section 200 to 600 m above the top of the Canol Formation (Tassonyi, 1969; Pugh, 1993; Dixon, 2012). In the Keele tectonic zone and south of it, similar limestone units are penetrated by wells at various distances above the Canol–Imperial contact, ranging from 150 to 2000 m (Pugh, 1993; Dixon, 2012), making assignment to a single stratigraphic unit unlikely. The Jungle Ridge Member was tied with the seismic reflector in the subsurface of the Mackenzie Plain north and south of the Keel Arch (MacLean, 2012). The laterally disappearing, westward shaling, and thinning character of the Jungle Ridge complies with its definition as a ‘lentic’ occurring at certain locations within the Imperial Formation clinoforms (Williams, 1989).

### ***Unit Cf***

Map ‘unit Cf’ (Norris, 1981) refers to the Famennian–Tournaisian dark grey siliceous shale mapped in the outcrops of the eastern Richardson Mountains, where it can reach up to 555 m in thickness (Allen et al., 2009, 2015). Unit Cf is age and facies equivalent to the Ford Lake Formation defined in the Kandik Basin of eastern Alaska–western Yukon (Brabb, 1969) and traced across north-central Yukon as ‘unit CF’ (Pugh, 1983; Gordey and Makepeace, 2003; Allen et al., 2009, 2015). Unit Cf in the study area contains interbeds of coarse siliciclastic material and grades laterally into the Tuttle Formation (Pugh, 1983). Although not formally recognized in the subsurface (Fraser and Hogue, 2007), the unit has been matched to discrete shale-dominated intervals in four exploration wells in the Yukon portion of the Peel Plateau (Allen et al., 2015). Shales of unit Cf are lithologically heterogeneous, ranging from organic-poor grey shale and siltstone to organic-rich fissile shale (‘wafery shale’ lithofacies) and black siliceous shale. Organic-carbon content in black-shale facies is high, keeping the average total organic carbon (TOC) value at 5.25 weight per cent. Kerogens are a mixture of Type II and Type III, with  $T_{\max}$  (~423°C–444°C) and  $R_o$  (~0.5%–0.95%) values indicating that maturity is within the oil window (Allen et al., 2015). Siliceous shales are brittle and rich in Type II organic matter, making them a potential high-quality shale-oil reservoir (Allen et al., 2015). Conditions that defined deposition and preservation of planktonic organic matter (precursor to Type II kerogen) may involve development of starved areas within the Ellesmerian foredeep (Lane, 2007) or phases in basin development when the rate of siliciclastic flux diminished. Synchronicity of the Ford Lake–Cf black-shale basin and the global development of anoxic shelf basins across the Devonian–Carboniferous boundary (Hangenberg–lower Alum black-shale events; Kaiser et al., 2015) is intriguing and prompts further research involving correlation with the time-equivalent Exshaw and Bakken formations of western Laurentia (Richards, 1989; Richards et al., 2002).

## CONSTRAINTS ON ORGANIC MATTER DEPOSITION AND PRESERVATION IN THE HORN RIVER GROUP

### Canol shale play

The Canol Formation has long been known as the source rock for the oil pool in the Norman Wells carbonate-bank reservoir (Snowdon et al., 1987; Yose et al., 2001; Hadlari, 2015). As of 2014, the Norman Wells oilfield had produced 274 million barrels of light oil since 1920 (National Energy Board – Northwest Territories Geological Survey, 2015), and production is currently on the decline. In recent years, the Canol Formation and underlying black-shale facies of the Horn River Group attracted investments into the Canol shale-play exploration (Indigenous and Northern Affairs Canada, 2014). Fourteen licences were granted between 2010 and 2013, for a total of \$627.5 million in work-bid commitments in the Mackenzie Valley (National Energy Board – Northwest Territories Geological Survey, 2015). Seven new exploration wells and two horizontal boreholes have been drilled. Despite an optimistic outlook on reservoir quality and estimated resource (Enachescu et al., 2013b), companies withdrew from exploration in early 2014 (Indigenous and Northern Affairs Canada, 2014). The reasons behind this withdrawal were stated as being related to climate conditions, lack of infrastructure and resultant pressure on operations costs, as well as land-regulation barriers (Wohlberg, 2014; Hogg, 2015).

Based on a representative set of inductively coupled plasma (ICP) elemental data from cores of Loon Creek O-06 and Little Bear N-09 wells, the Prohibition Creek–Canol interval in the SOB zone of the central Mackenzie Valley represents one brittle, siliceous, and partly carbonate-rich interval with low clay content (median Al ~3.4–4.3 weight per cent, median SiO<sub>2</sub> ~67–76 weight per cent) and median TOC (5–5.3 weight per cent; Kabanov and Gouwy, 2017; Kabanov, 2019); this low clay content was confirmed by X-ray diffraction data (Kabanov et al., 2016d). The Bluefish Member has an elevated clay content (median Al 5.4 weight per cent) and high TOC (5.1 weight per cent). Reservoir properties of the lower Loon Creek Member may be also fairly good, as indicated by the median values registered for Al (5.4 weight per cent), SiO<sub>2</sub> (69 weight per cent), and TOC (3 weight per cent). The three potential shale-reservoir horizons are separated by ductile, clay-rich shales of the Francis Creek and Mirror Lake members. Two main pay horizons were recognized by MGM Energy, corresponding to the Bluefish and Canol shales, each having a total shale porosity of approximately 8% and higher (Enachescu et al., 2013a, b; Hogg, 2015). In the Mackenzie Plain Petroleum Project area of the Northwest Territories Geological Survey (NTGS; Pyle et al., 2014), the probabilistic resource assessment for liquid hydrocarbon gave an estimate of 82.6 to 220.6 billion barrels

of oil-in-place for the Canol shale and 27.6 to 70.8 billion barrels for the Bluefish, making this a giant prospect, even if the recoverable resource does not exceed 1% (National Energy Board – Northwest Territories Geological Survey, 2015). This estimate does not take into account the higher level of maturity in a large part of the Mackenzie Valley synclinorium, where the Horn River Group occurs in the gas window and possibly beyond (Pyle et al., 2015; Kabanov, 2017b). Acceptance of recent changes in formation tops (Kabanov et al., 2016a; Kabanov and Deblonde, 2019) will also lead to corrections in resource estimates. The formation top picking of lithostratigraphic units proposed by Kabanov and Deblonde (2019) has changed unit thicknesses quite significantly. For example, a major change in the Canol Formation top in excess of 15 m occurs in 26 out of 55 wells within the Mackenzie Plain Petroleum Project area of the NTGS (Pyle et al., 2014). The lower portion of the Loon Creek Member is delineated as a potential 10 to 15 m thick pay zone, as observed in the East MacKay I-77 and I-78 wells (Enachescu et al., 2013a, b; Hogg, 2015), and a separate reservoir evaluation should be considered for it, since well-to-well correlation is established (Kabanov and Gouwy, 2017).

### Thermal maturity and burial history

The conventional petroleum model for the Norman Wells oilfield involves peak maturation of the Canol source rock during the Late Cretaceous–Tertiary under the Laramide clastic load (Snowdon et al., 1987; Gal et al., 2009). However, this model does not explain the absence of oil discoveries in other carbonate banks of the Ramparts Formation (Hadlari, 2015). Recent thermochronology data suggest that the burial–exhumation history might have been more complex. The vitrinite reflectance log and apatite fission-track thermal-history model from the East McKay I-77 well in the SOB zone indicated a pre-Cretaceous heating of Devonian rocks, with the greatest burial and maturation rates likely occurring in the Triassic to Middle Jurassic (Issler et al., 2005). Recently obtained apatite and zircon (U-Th)/He data from the Mackenzie Plain allow reconstruction of maximum burial of the Imperial Formation up to 120°C to 160°C during the Pennsylvanian–Late Triassic (Powell, 2017). Laramide foreland load in these models buried Imperial Formation strata to depths between 2.2 and 3.8 km at a temperature of about 100°C, which would not overprint the late Paleozoic–early Mesozoic maximum-burial trend. The apatite (U-Th)/He evidence for kilometre-scale erosion of late Paleozoic–early Mesozoic sedimentary rocks is strong, as it extends beyond the Mackenzie Plain to the adjacent Mackenzie Mountains (Powell et al., 2016) and the western portion of the Canadian Shield (Ault et al., 2013).

Hadlari (2015) proposed a new petroleum model consistent with thermochronology-based burial–unroofing history. In this model, oil in the Norman Wells reservoir is the second, very recent charge into the overall overmature system;



injection of oil into the reservoir was possible under a unique condition of the actively exhuming hanging wall of the Mackenzie Valley synclinorium. Uplift-related decompression transferred the Canol siliceous mudrock from a ductile to a brittle state, which in combination with tectonic stress enhanced natural fracturing, leading to the release of residual light oil into the reservoir (Hadlari, 2015). However, Canol kerogens occur in the oil window not only at the Norman Wells reservoir but in the larger zone trending for approximately 180 km along the Franklin Mountains side of the Mackenzie Valley to the Keele tectonic zone (Pyle et al., 2015). In other parts of the study area, mudrocks of the Horn River Group occur in the gas window and beyond (Pyle et al., 2015; Kabanov, 2017b). The zone of low thermal maturity is characterized by  $T_{\max}$  values of 426°C to 445°C (Pyle et al., 2015) and colour alteration indices of 1.5 to 2.0 (S. Gouwy, unpub. rept., 2016). The vitrinite-reflectance and bitumen-equivalent parameter  $R_o$  corresponds to an advanced level of maturity, when compared to the  $T_{\max}$  values, but consistently less mature than in surrounding areas (Pyle et al., 2015). Good preservation of biomarker species in the Canol and Hare Indian shales within this zone (Jiang et al., 2020; Kabanov and Jiang, 2020) indicates that this is a primary zone that has never experienced advanced breakdown of particulate organic matter. This low-maturity zone seemingly fits into the Laramide structural layout, which cannot be reconciled with advanced pre-Laramide cooking inferred from the thermochronology models of Issler et al. (2005) and Powell (2017).

## Oceanographic control on deposition of organic matter

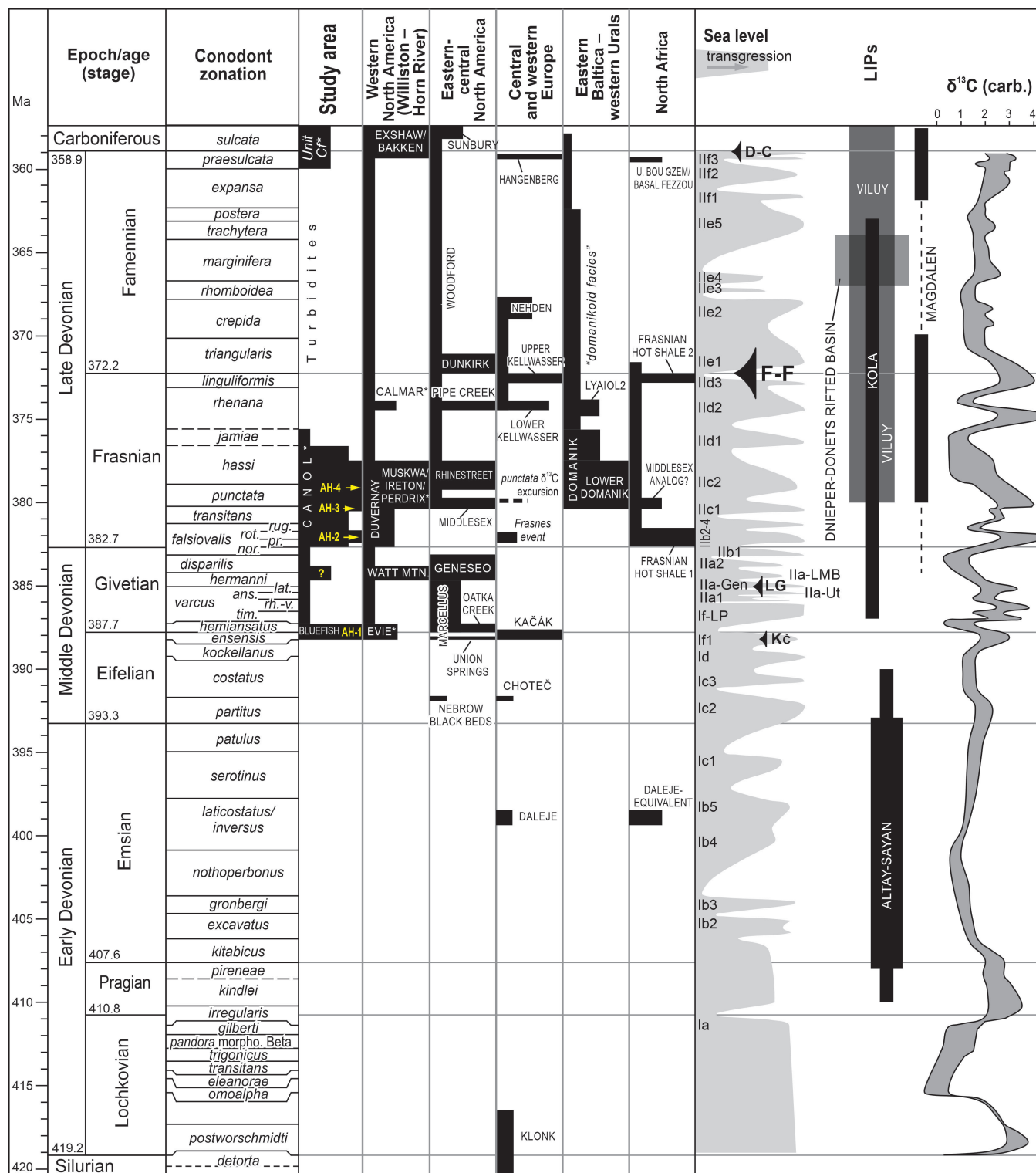
Planktonogenic alginite-rich organic matter precursor to oils and types I and II kerogens (Peters and Cassa, 1994) is preserved in settings where a shallow chemocline separates oxic and anoxic waters at or above the sediment–water interface, allowing rapid removal of particulate organic matter from the zone of aerobic remineralization into an anoxic environment (Arthur and Sageman, 1994; Burdige, 2007).

This statement encompasses diverse basins in which organic matter accumulates in multicomponent systems, ranging from overproduction in eutrophic settings in west-coast upwelling zones to less productive landlocked basins, where a shallow permanent chemocline ensures the high preservation potential of organic particles (Arthur and Sageman, 1994, 2005).

The Horn River Group of the study area is essentially a northern continuation of the Devonian–Lower Mississippian source rock trend of the Western Canada Sedimentary Basin (Creaney et al., 1994; Hamblin, 2006). Source rock depositional environments in this vast swath of shelf seaways have not been the subject of much research. Extreme spreads of anoxic sediments during the second half of the Devonian tend to correlate in many shelf basins of the world and, therefore, are frequently referred to as the ‘Devonian anoxic or black-shale events’ (Fig. 6). These anoxic events are conventionally seen as a result of genuine deepening or global eustatic transgressions (Johnson et al., 1985; Sandberg et al., 2002; Arthur and Sageman, 2005; Brett et al., 2011), but the debate continues over the shortage of rigorous evidence for sea-level changes (Bond and Wignall, 2008; Kabanov and Jiang, 2020; Racki, 2020). It appears, on the other hand, that fluctuating global ocean-redox state seems alone to be able to govern simultaneous shifts to anoxic facies, coupled or not with sea-level changes (Meyer and Kump, 2008), as clearly demonstrated by the periods of anoxic sedimentation in Mesozoic greenhouse oceans, culminating in oceanic anoxic events (OAEs; Jenkyns, 2010).

Kabanov (2019) recognized four main horizons of enhanced anoxia (AHs; Fig. 6) within the Horn River Group of the central Mackenzie Valley. Aluminum-normalized Mo and U logs in two cored sections revealed the AH-I close to the Eifelian–Givetian boundary, AH-II in the basal Frasnian, and AH-III and AH-IV bundled in the middle Frasnian interval (Fig. 6). These four horizons are characterized by attenuated siliciclastic components (Kabanov, 2019) and are also expressed as positive  $\delta^{13}C_{org}$  excursions (Kabanov and Jiang, 2020). In outcrops, AHs can be traced with gamma-ray spectrometry, with the most useful results provided by the

**Figure 6.** Black shales of the Horn River Group in the study area correlated with counterparts in five global regions on the chart of post-Lochkovian Devonian (*modified from* Kabanov and Jiang, 2020). Yellow labels denote main anoxic horizons (AHs) of the Horn River Group. Right column: sea-level curve and  $\delta^{13}C$  curve from skeletal carbonate (carb.) are redrawn *from* Becker et al. (2012); prominent biotic crises as *compiled by* Bond and Grasby (2017); age ranges of large igneous provinces (LIPs) are *from* Kravchinsky (2012), Bond and Wignall (2014), and Racki (2020). The depopphase indexing on the sea-level curve is *from* Johnson et al. (1985). Marine biotic crises (arrow size reflects severity): Frasnian–Famennian (F–F), end-Devonian or Devonian–Carboniferous (D–C), late Givetian (LG), and late Eifelian or Kačák (Kč). Width of the LIP bars reflects the relative interpreted volume of emplaced basalts. Alternative Givetian–Frasnian conodont zones *timorensis* (*tim.*), *rhenanus-varcus* (*rh.-v.*), *ansatus* (*ans.*), *latifossatus/semialternans* (*lat.*), *norrissi* (*nor.*), *pristina* (*pr.*), *rotundiloba* (*rot.*), and *rugosa* (*rug.*) are *from* Narkiewicz and Bultynck (2007) and Becker et al. (2016). Asterisks (\*) denote units with notably poor age control. Calibration of radiometric ages from Geologic Time Scale 2012 (Becker et al., 2012).



uranium-stripped, potassium–thorium response and U-based proxies for authigenic metal enrichment (Kabanov, 2019; Kabanov and Deblonde, 2019). The AHs are biostratigraphically correlated with black-shale events in several basins of the world (Fig. 6). Based on ICP elemental data from a representative set of 1687 samples, siliciclastic-lean basinal mudrock units that host AHs are strongly enriched in Mo compared to siliciclastic-rich units and show strong U/Mo covariation ( $r \approx 0.8$ ; Kabanov, 2019). Supported by a lack of geological evidence for an oceanographic barrier, this enrichment indicates unrestricted water exchange with Panthalassa. At the same time, development of oligotrophy is indicated by a lack of phosphorus enrichment and weak to nonexistent enrichment in Zn and Cu (Kabanov, 2019). These features can be reconciled through the conceptual model of Kidder and Worsley (2010), which involves a global shift to a warm greenhouse mode with slowed oceanic convection, expanded oxygen-minimum zones (OMZs), and a failure of nutrient resupply from the upwelling. The onset of mass degassing in continental large igneous provinces, probably combined with the enhanced eruptive activity in oceanic arcs, represents a potential trigger for this mid-Devonian shift (Bond and Wignall, 2014; Racki, 2020). Other explanations exist, such as eutrophication of the ocean caused by a boost in soil erosion during land afforestation (Algeo et al., 1995). Devonian black-shale events may represent genuine OAEs. However, unequivocal assignment to OAEs is curtailed by a lack of sufficient evidence for nutrient and trace-metal crises. A fully developed OAE-inducing hothouse crisis is predicted to show a negative swing of  $\delta^{13}\text{C}_{\text{carb}}$  and  $\delta^{13}\text{C}_{\text{org}}$  caused by a drop in primary production as a result of nutrient arrest in expanded OMZs (Kidder and Worsley, 2010; Grasby et al., 2016). Some horizons of fully developed OAEs also record negative excursions of Mo, U, and Zn, which is probably a response to the drawdown of oceanic inventories of these metals by enhanced precipitation in expanded anoxic waters (Algeo and Rowe, 2012). These negative swings of trace metals are not observed in the Horn River Group (Kabanov, 2019). The Devonian black-shale events typically respond by overall positive  $\delta^{13}\text{C}$  excursions imprinted in skeletal carbonate units and organic matter (Joachimski et al., 2002; Kidder and Worsley, 2010), which is also the case in the Canol Formation and the Horn River Group of the study area (Fraser and Hutchison, 2017; Kabanov and Jiang, 2020).

It is therefore clear that the oceanographic control on the organic-matter deposition in Devonian source rocks of the study area, as well as in homotaxial source rocks of the Western Canada Sedimentary Basin, cannot be ascribed solely to sea-level fluctuations, which in fact may not be the main factor at all (Kabanov and Jiang, 2020). A consistent model has yet to be developed through understanding of rather nonactualistic Earth-surface processes of the middle Paleozoic projected into simultaneous black-shale events in remote shelf basins.

## CONCLUDING REMARKS

The Devonian System of the Mackenzie Corridor is a stratigraphic succession of past, present, and likely future economic importance. In the study area located between latitudes 64.5°N and 68°N, the economic prospectivity is tied to the major total petroleum system of the latest Eifelian–Frasnian Horn River Group. Organic-rich mudrocks of the Horn River Group sourced hydrocarbons to the Norman Wells and Summit Creek conventional oilfields (Hannigan et al., 2011). Much larger, technologically recoverable oil and gas resources are locked in the Horn River Group source rocks, also known as the Canol shale play (National Energy Board – Northwest Territories Geological Survey, 2015). In the western corner of the study area corresponding mostly to the Peel Plateau, the Famennian–Tournaisian shales of the informal map unit Cf (equivalent of the Ford Lake Formation) may also represent an excellent oil-prone source rock (Allen et al., 2015), but remoteness and absence of infrastructure preclude this asset from being economically viable at present.

Progress achieved on the Horn River Group in recent decades includes a drastic increase in the publicly available database on elemental geochemistry, organic-richness, and thermal-maturity proxies, as well as mineral composition. An upgraded lithostratigraphic framework and improved correlation in the subsurface aim to put more accuracy on the geometry of pay units (Kabanov and Gouwy, 2017; Kabanov and Deblonde, 2019). Acquisition of a large volume of analytical data and recent lithostratigraphic updates may be used for future resource reassessment. Several gaps in fundamental knowledge also remain. First, the burial–exhumation history of Devonian rocks is controversial, specifically in the Mackenzie Valley, with conflicting lines of evidence provided by thermochronology, thermal-maturity parameters, and organic geochemistry. Second, there is a lack of age constraints on the Canol Formation, especially its upper part and the top (Kabanov and Gouwy, 2017; Gouwy, this volume). Third, factors that governed large-scale deposition and preservation of organic matter during the second half of the Devonian are poorly understood, not only in the study area, but across the entire Western Canada Sedimentary Basin and on a global scale.

The underlying part of the Devonian succession is dominated by shallow-water carbonate units and evaporites. Progress achieved in recent years includes recognition of dozens of stacked subaerial exposure surfaces bundling shallow-water peritidal cycles or parasequences in the Arnica and Landry formations. Some subaerial surfaces bear rubbly pedogenic horizons and many metres of vadose dissolution features underneath, indicating protracted development. On the other hand, the surface at the base of the Delorme Group, long referred to as a major sub-Devonian unconformity, is concordant with no conclusive evidence of advanced subaerial alteration across the study area, although an angular



unconformity at this level occurs locally farther south. This promotes the need for greater scrutiny of the sequence-stratigraphic architecture of the Early Devonian–Eifelian strata, including more accurate assessment and ranking of unconformities and facies successions.

## ACKNOWLEDGMENTS

The Devonian Stratigraphic Framework study is part of the Mackenzie project of the Geo-mapping for Energy and Minerals (GEM-2) program, with management support provided by Carl Ozyer, Marlene Francis, and Paul Wozniak of the Geological Survey of Canada (GSC). The scientific content of this paper improved substantially through the critical reviews by Thomas Hadlari and David Morrow (GSC), and its final quality gained from editing by Marie-France Dufour and Natalie Morisset. Instances of help with this study are countless: the most significant and versatile help was provided by GSC colleagues Sofie Gouwy, Robert MacNaughton, and Karen Fallas; students Damien Weleschuk and Wing Chuen Chan (hired as part of the Federal Student Work Experience Program); GSC lab assistants Shishua (Wendy) Zhao and Mary Luz Borrero Gomez; Richard Fontaine and William Dwyer of the GSC Core and Sample facility; and especially Richard Vandenberg (GSC). Tremendous progress in acquiring new analytical data during the 2014 to 2019 period would not have been achievable without the prompt approvals for sampling issued by the Canada Energy Regulator (authorizations no. 12599, 12609, 12616, 12619, 12624, and 12632) and the Office of the Regulator of Oil and Gas Operations in the Northwest Territories (SR-2017-003 and SR-2017-004). The author also expresses his gratitude to Brad Harvey (GSC) for deploying and servicing the RSA-230 tool; and Pierre Pelchat, Andy Mort (both GSC), and Michelle Cameron (Bruker Elemental), who helped deploy and set up the Bruker Tracer IV instrument. This work is a contribution to the IGCP-652 Project “Reading geologic time in Paleozoic sedimentary rocks”.

## REFERENCES

- Aitken, J.D., Cook, D.G., and Yorath, C.J., 1982. Upper Ramparts River (106G) and Sans Sault Rapids (106H) map areas, District of Mackenzie; Geological Survey of Canada, Memoir 388, 48 p. <https://doi.org/10.4095/116165>
- Algeo, T.J. and Rowe, H., 2012. Paleoceanographic applications of trace-metal concentration data; *Chemical Geology*, v. 324–325, p. 6–18. <https://doi.org/10.1016/j.chemgeo.2011.09.002>
- Algeo, T.J., Berner, R.A., Maynard, J.B., and Scheckler, S.E., 1995. Late Devonian oceanic anoxic events and biotic crises: “Rooted” in the evolution of vascular land plants; *Geological Society of America, GSA Today*, v. 5, p. 64–66.
- Allen, T.L., Fraser, T.A., and Utting, J., 2009. Upper Devonian to Carboniferous strata II — Tuttle Formation play; Chapter 8 in *Regional geoscience studies and petroleum potential, Peel Plateau and Plain, Northwest Territories and Yukon*, Project Volume, (ed.) L.J. Pyle and A.L. Jones; Northwest Territories Geoscience Office and Yukon Geological Survey, NWT Open File 2009-02 and YGS Open File 2009-25, p. 365–409.
- Allen, T.L., Fraser, T.A., Hutchison, M.P., Dolby, G., Reyes, J., and Utting, J., 2015. Stratigraphy, age, and petroleum potential of Upper Devonian black shale (unit ‘Cf’), east Richardson Mountains and Peel Plateau, Yukon; Yukon Geological Survey, Open File 2015-3, 55 p.
- Arthur, M.A. and Sageman, B.B., 1994. Marine black shales: depositional mechanisms and environments of ancient deposits; *Annual Review of Earth and Planetary Sciences*, v. 22, p. 499–551. <https://doi.org/10.1146/annurev.ea.22.050194.002435>
- Arthur, M.A. and Sageman, B.B., 2005. Sea-level control on source-rock development: perspectives from the Holocene Black Sea, the mid-Cretaceous Western Interior Basin of North America, and the Late Devonian Appalachian Basin; in *The deposition of organic-carbon-rich sediments: models, mechanisms, and consequences*, (ed.) N.B. Harris; Society for Sedimentary Geology, SEPM Special Publication 82, p. 35–59. <https://doi.org/10.2110/pec.05.82.0035>
- Ault, A.K., Flowers, R.M., and Bowring, S.A., 2013. Phanerozoic surface history of the Slave craton; *Tectonics*, v. 32, p. 1066–1083. <https://doi.org/10.1002/tect.20069>
- Bassett, H.G., 1961. Devonian stratigraphy, central Mackenzie River region, Northwest Territories, Canada; in *Geology of the Arctic: Proceedings of the First International Symposium of Arctic Geology*, (ed.) G.O. Raasch; University of Toronto Press, v. 1, p. 481–498. <https://doi.org/10.3138/9781487584979-043>
- Becker, R.T., Gradstein, F.M., and Hammer, O., 2012. The Devonian Period; Chapter 22 in *The geologic time scale 2012*, (ed.) F.M. Gradstein, J.G. Ogg, M. Schmitz, and G. Ogg; Elsevier, Amsterdam, v. 2, p. 559–601. <https://doi.org/10.1016/B978-0-444-59425-9.00022-6>
- Becker, R.T., Königshof, P., and Brett, C.E., 2016. Devonian climate, sea level and evolutionary events: an introduction; in *Devonian climate, sea level and evolutionary events*, (ed.) R.T. Becker, P. Königshof, and C.E. Brett; Geological Society of London, Special Publications, v. 423, p. 1–10. <https://doi.org/10.1144/SP423.15>
- Belyea, H.R., 1970. Significance of an unconformity within the Chinchaga Formation, northern Alberta, and northeastern British Columbia; in *Report of activities, Part B; Geological Survey of Canada, Paper 70-1B*, p. 76–79. <https://doi.org/10.4095/105680>
- Beranek, L.P., Mortensen, J.K., Lane, L., Allen, T., Fraser, T., Hadlari, T., and Zantvoort, W.G., 2010. Detrital zircon geochronology of the western Ellesmerian clastic wedge, northwestern Canada: insights on Arctic tectonics and evolution of the northern Cordilleran miogeocline; *Geological Society of America, Bulletin*, v. 122, p. 1899–1911. <https://doi.org/10.1130/B30120.1>

- Bond, D.P.G. and Grasby, S.E., 2017. On the causes of mass extinctions; Palaeogeography, Palaeoclimatology, Palaeoecology, v. 478, p. 3–29. <https://doi.org/10.1016/j.palaeo.2016.11.005>
- Bond, D.P.G. and Wignall, P.B., 2008. The role of sea-level change and marine anoxia in the Frasnian–Famennian (Late Devonian) mass extinction; Palaeogeography, Palaeoclimatology, Palaeoecology, v. 263, p. 107–118. <https://doi.org/10.1016/j.palaeo.2008.02.015>
- Bond, D.P.G. and Wignall, P.B., 2014. Large igneous provinces and mass extinctions: an update; in *Volcanism, impacts, and mass extinctions: causes and effects*, (ed.) G. Keller and A.C. Kerr; Geological Society of America, Special Paper, v. 505, p. 29–55. [https://doi.org/10.1130/2014.2505\(02\)](https://doi.org/10.1130/2014.2505(02))
- Brabb, E.E., 1969. Six new Paleozoic and Mesozoic formations in east-central Alaska; United States Geological Survey, Bulletin 1274-I, 26 p.
- Braman, D.R. and Hills, L.V., 1992. Upper Devonian–lower Carboniferous miospores, western District of Mackenzie and Yukon Territory, Canada; *Paleontographica Canadiana*, v. 8, p. 1–97.
- Braun, W.K., 1966. Stratigraphy and microfauna of Middle and Upper Devonian formations, Norman Wells area, Northwest Territories, Canada; *Neues Jahrbuch für Geologie und Paläontologie*, v. 125, p. 247–264.
- Brett, C.E., Baird, G.C., Bartholomew, A.J., DeSantis, M.K., and Ver Straeten, C.A., 2011. Sequence stratigraphy and a revised sea-level curve for the Middle Devonian of eastern North America; Palaeogeography, Palaeoclimatology, Palaeoecology, v. 304, p. 21–53. <https://doi.org/10.1016/j.palaeo.2010.10.009>
- Burdige, D.J., 2007. Preservation of organic matter in marine sediments: controls, mechanisms, and an imbalance in sediment organic carbon budgets; *Chemical Reviews*, v. 107, p. 467–485. <https://doi.org/10.1021/cr050347q>
- Catuneanu, O., 2006. Principles of sequence stratigraphy; Elsevier, Amsterdam, 375 p. <https://doi.org/10.1017/S0016756807003627>
- Cecile, M.P., Hutcheon, I.E., and Gardner, D., 1982. Geology of the northern Richardson anticlinorium; Geological Survey of Canada, Open File 875, scale 1:125 000. <https://doi.org/10.4095/129759>
- Cecile, M.P., Morrow, D.W., and Williams, G.K., 1997. Early Paleozoic (Cambrian to Early Devonian) tectonic framework, Canadian Cordillera; *Bulletin of Canadian Petroleum Geology*, v. 45, no. 1, p. 54–74.
- Chatterton, B.D.E., 1978. Aspects of late Early and Middle Devonian conodont biostratigraphy of western and northwest Canada; in *Western and Arctic Canadian biostratigraphy*, (ed.) C.R. Stelck and B.D.E. Chatterton; Geological Association of Canada, Special Paper 18, p. 161–231.
- Cohen, K.M., Finney, S.C., Gibbard, P.L., and Fan, J.-X., 2013. The ICS international chronostratigraphic chart (updated), v2018; Episodes, v. 36, p. 199–204. <http://www.stratigraphy.org/ICSchart/ChronostratChart2018-08.pdf> [accessed January 29, 2020]
- Cook, D.G., 1975. The Keele Arch — a pre-Devonian and pre-Late Cretaceous paleo-upland in the northern Franklin Mountains and Colville Hills; in *Report of activities, Part C*; Geological Survey of Canada, Paper 75-1C, p. 243–246. <https://doi.org/10.4095/103077>
- Cook, D.G. and MacLean, B.C., 1993. Revised bedrock geology of Belot Ridge, District of Mackenzie, Northwest Territories; in *Current research, Part B*; Geological Survey of Canada, Paper 93-1B, p. 33–38. <https://doi.org/10.4095/134220>
- Corlett, H. and Jones, B., 2011. The influence of paleogeography in epicontinental seas: a case study based on Middle Devonian strata from the MacKenzie Basin, Northwest Territories, Canada; *Sedimentary Geology*, v. 239, p. 199–216. <https://doi.org/10.1016/j.sedgeo.2011.07.001>
- Creaney, S., Allan, J., Cole, K.S., Fowler, M.G., Brooks, P.W., Osadetz, K.G., Macqueen, R.W., Snowdon, L.R., and Riediger, C.L., 1994. Petroleum generation and migration in the Western Canada Sedimentary Basin; Chapter 31 in *Geological atlas of the Western Canada Sedimentary Basin*, (comp.) G.D. Mossop and I. Shetsen; Canadian Society of Petroleum Geologists and Alberta Research Council, Calgary, p. 455–468.
- Dewing, K. and Embry, A.F., 2007. Geological and geochemical data from the Canadian Arctic Islands. Part I: Stratigraphic tops from Arctic Islands’ oil and gas exploration boreholes; Geological Survey of Canada, Open File 5442, 7 p. <https://doi.org/10.4095/223386>
- Dewing, K., Sharp, R.J., Ootes, L., Turner, E.C., and Gleeson, S., 2006. Geological assessment of known Zn-Pb showings, Mackenzie Mountains, Northwest Territories; Geological Survey of Canada, Current Research 2006-A4, 12 p. <https://doi.org/10.4095/222108>
- Dixon, J., 2012. Subsurface correlations in the Upper Devonian to lower Carboniferous clastic wedge (Imperial and Tuttle formations), Northwest Territories; Geological Survey of Canada, Open File 6862, 51 p. <https://doi.org/10.4095/289618>
- Douglas, R.J.W. and Norris, D.K., 1961. Camsell Bend and Root River map areas, Northwest Territories (95 J, K); Geological Survey of Canada, Paper 61-13, 41 p. <https://doi.org/10.4095/101102>
- Douglas, R.J.W. and Norris, D.K., 1977. Geology, Virginia Falls, District of Mackenzie; Geological Survey of Canada, Map 1378A, scale 1:250 000. <https://doi.org/10.4095/109052>
- Embry, A.E. and Klovan, J.E., 1976. The Middle–Upper Devonian clastic wedge of the Franklinian geosyncline; *Bulletin of Canadian Petroleum Geology*, v. 24, p. 485–639.
- Enachescu, M.E., Kierulf, F., Price, P., Cooper, M., and Châtenay, A., 2013a. Geophysical characterization of the Canol and Bluefish oil shales, central Mackenzie Valley, NWT, Canada; GeoConvention 2013: Integration; Canadian Society of Petroleum Geologists, extended abstracts. [https://www.cspg.org/cspg/Conferences/Geoconvention/2013\\_Abstract\\_Archives.aspx](https://www.cspg.org/cspg/Conferences/Geoconvention/2013_Abstract_Archives.aspx) [accessed May 13, 2017]

- Enachescu, M.E., Price, P.R., Hogg, J.R., Kierulf, F., Cooper, M.F.J., and Springer, A.C., 2013b. Geological, geochemical and geophysical characteristics of the Devonian oil shales in central Mackenzie Valley, NWT, Canada; Annual Convention and Exhibition, American Association of Petroleum Geologists, Search and Discovery Article #10559. <[https://www.searchanddiscovery.com/documents/2013/10559enachescu/ndx\\_enachescu.pdf](https://www.searchanddiscovery.com/documents/2013/10559enachescu/ndx_enachescu.pdf)> [accessed May 1, 2019]
- Fallas, K.M., 2013a. Geology, Norman Wells (northwest), Northwest Territories; Geological Survey of Canada, Canadian Geoscience Map 98, scale 1:100 000. <https://doi.org/10.4095/292290>
- Fallas, K.M., 2013b. Geology, Norman Wells (northeast), Northwest Territories; Geological Survey of Canada, Canadian Geoscience Map 99, scale 1:100 000. <https://doi.org/10.4095/292291>
- Fallas, K.M., 2018a. Bedrock geology, Lac des Bois, Northwest Territories; Geological Survey of Canada, Canadian Geoscience Map 308, scale 1:250 000. <https://doi.org/10.4095/306201>
- Fallas, K.M., 2018b. Bedrock geology, Lac Belot, Northwest Territories; Geological Survey of Canada, Canadian Geoscience Map 309, scale 1:250 000. <https://doi.org/10.4095/306202>
- Fallas, K.M., 2018c. Bedrock geology, Aubry Lake, Northwest Territories; Geological Survey of Canada, Canadian Geoscience Map 310, scale 1:250 000. <https://doi.org/10.4095/306203>
- Fallas, K.M., 2018d. Bedrock geology, Lac Maunoir, Northwest Territories; Geological Survey of Canada, Canadian Geoscience Map 311, scale 1:250 000. <https://doi.org/10.4095/306205>
- Fallas, K.M. and MacNaughton, R.B., 2013. Geology, Norman Wells (southeast), Northwest Territories; Geological Survey of Canada, Canadian Geoscience Map 100, scale 1:100 000. <https://doi.org/10.4095/292292>
- Fallas, K.M. and MacNaughton, R.B., 2020a. Bedrock geology, Sans Sault Rapids southwest, Northwest Territories (NTS 106H/SW); Geological Survey of Canada, Canadian Geoscience Map 420, scale 1:100 000. <https://doi.org/10.4095/314794>
- Fallas, K.M. and MacNaughton, R.B., 2020b. Bedrock geology, Sans Sault Rapids southeast, Northwest Territories (NTS 106H/SE); Geological Survey of Canada, Canadian Geoscience Map 421, scale 1:100 000. <https://doi.org/10.4095/314787>
- Fallas, K.M., MacNaughton, R.B., MacLean, B.C., and Hadlari, T., 2013. Geology, Norman Wells (southwest), Northwest Territories; Geological Survey of Canada, Canadian Geoscience Map 101, scale 1:100 000. <https://doi.org/10.4095/292293>
- Fallas, K.M., MacNaughton, R.B., and Sommers, M.J., 2015. Maximizing the value of historical bedrock field observations: an example from northwest Canada; *GeoResJ*, v. 6, p. 30–43. <https://doi.org/10.1016/j.grj.2015.01.004>
- Fallas, K.M., MacNaughton, R.B., Hannigan, P.K., and MacLean, B.C., 2021. Mackenzie–Peel Platform and Ellesmerian foreland composite tectono-sedimentary element, northwestern Canada; *in* Sedimentary successions of the Arctic region and their hydrocarbon prospectivity, (ed.) S.S. Drachev, H. Brekke, E. Henriksen, and T. Moore; Geological Society of London, Memoir 57. <https://doi.org/10.1144/M57-2016-5>
- Fraser, T.A., 2014. Field descriptions of the Middle–Upper Devonian Canol Formation on Trail River, east Richardson Mountains, Yukon; *in* Yukon exploration and geology 2013, (ed.) K.E. MacFarlane, M.G. Nordling, and P.J. Sack; Yukon Geological Survey, p. 53–68.
- Fraser, T.A. and Allen, T.L., 2007. Field investigations of the Upper Devonian to lower Carboniferous Tuttle Formation, eastern Richardson Mountains, Yukon; *in* Yukon exploration and geology 2006, (ed.) D.S. Emond, L.L. Lewis, and L.H. Weston, Yukon Geological Survey, p. 157–173.
- Fraser, T. and Hogue, B., 2007. List of wells and formation tops, Yukon Territory, version 1.0; Yukon Geological Survey, YGS Open File 2007-5, 1 p. plus spreadsheet.
- Fraser, T.A. and Hutchison, M.P., 2017. Lithogeochemical characterization of the Middle–Upper Devonian Road River Group and Canol and Imperial formations on Trail River, east Richardson Mountains, Yukon: age constraints and a depositional model for fine-grained strata in the lower Paleozoic Richardson trough; *Canadian Journal of Earth Sciences*, v. 54, p. 731–765. <https://doi.org/10.1139/cjes-2016-0216>
- Fraser, T.A., Crawford, I., Gadd, M.G., Henderson, K., Layton-Matthews, D., Melchin, M., Peter, J.M., Sack, P.J., Sperling, E., and Strauss, J., 2017. An overview of shale studies in Yukon during 2017 field season; *in* Yukon exploration and geology 2017, (ed.) K.E. MacFarlane; Yukon Geological Survey, p. 37–45.
- Gadd, M.G. and Peter, J.M., 2018. Field observations, mineralogy and geochemistry of Middle Devonian Ni–Zn–Mo–PGE hyper-enriched black shale deposits, Yukon; *in* Targeted Geoscience Initiative: 2017 report of activities, volume 1, (ed.) N. Rogers; Geological Survey of Canada, Open File 8358, p. 193–206. <https://doi.org/10.4095/306475>
- Gadd, M.G., Peter, J.M., Hnatyshin, D., Creaser, R., Gouwy, S., and Fraser, T., 2020. A Middle Devonian basin-scale precious metal enrichment event across northern Yukon (Canada); *Geology*, v. 48, p. 242–246. <https://doi.org/10.1130/G46874.1>
- Gal, L.P. and Pyle, L.J., 2009. Upper Silurian–Lower Devonian strata (Delorme Group); Chapter 5 *in* Regional geoscience studies and petroleum potential, Peel Plateau and Plain, Northwest Territories and Yukon, Project Volume, (ed.) L.J. Pyle and A.L. Jones; Northwest Territories Geoscience Office and Yukon Geological Survey, NWT Open File 2009-02 and YGS Open File 2009-25, p. 161–186.
- Gal, L.P., Pyle, L.J., Hadlari, T., and Allen, T.L., 2009. Lower to Upper Devonian strata, Arnica–Landry Play, and Kee Scarp Play; Chapter 6 *in* Regional geoscience studies and petroleum potential, Peel Plateau and Plain, Northwest Territories and Yukon, Project Volume, (ed.) L.J. Pyle and A.L. Jones; Northwest Territories Geoscience Office and Yukon Geological Survey, NWT Open File 2009-02 and YGS Open File 2009-25, p. 187–289.



- Gordey, S.P. and Makepeace, A.J. (comp.), 2003. Yukon digital geology; Geological Survey of Canada, Open File 1749 (edited version 2) and Yukon Geology Program, Open File 2003-9(D), scale 1:1 000 000. <https://doi.org/10.4095/214639>
- Gouwy, S.A., MacNaughton, R.B., and Fallas, K.M., 2017. New conodont data constraining the age of the 'Bear Rock assemblage' in the Colville Hills, Northwest Territories; Geological Survey of Canada, Current Research 2017-3, 11 p. <https://doi.org/10.4095/306171>
- Grasby, S.E., Beauchamp, B., and Knies, J., 2016. Early Triassic productivity crises delayed recovery from world's worst mass extinction; *Geology*, v. 44, p. 779–782. <https://doi.org/10.1130/G38141.1>
- Hadlari, T., 2015. Oil migration driven by exhumation of the Canol Formation oil shale: a new conceptual model for the Norman Wells oil field, northwestern Canada; *Marine and Petroleum Geology*, v. 65, p. 172–177. <https://doi.org/10.1016/j.marpetgeo.2015.03.027>
- Hadlari, T., Gal, L.P., Zantvoort, W.G., Tylosky, S.A., Allen, T.L., Fraser, T.A., Lemieux, Y., and Catuneanu, O., 2009a. Upper Devonian to Carboniferous strata I — Imperial Formation play; in *Regional geoscience studies and petroleum potential, Peel Plateau and Plain, Northwest Territories and Yukon*, Project Volume, (ed.) L.J. Pyle and A.L. Jones; Northwest Territories Geoscience Office and Yukon Geological Survey, NWT Open File 2009-02 and YGS Open File 2009-25, p. 290–364.
- Hadlari, T., Tylosky, S.A., Lemieux, Y., Zantvoort, W.G., and Catuneanu, O., 2009b. Slope and submarine fan turbidite facies of the Upper Devonian Imperial Formation, northern Mackenzie Mountains, NWT; *Bulletin of Canadian Petroleum Geology*, v. 57, p. 192–208. <https://doi.org/10.2113/gscpgbull.57.2.192>
- Hamblin, A.P., 2006. The "shale gas" concept in Canada: a preliminary inventory of possibilities; Geological Survey of Canada, Open File Report 5384, 108 p. <https://doi.org/10.4095/222641>
- Hannigan, P.K., Morrow, D.W., and MacLean, B.C., 2011. Petroleum resource potential of the northern mainland of Canada (Mackenzie Corridor); Geological Survey of Canada, Open File 6757, 271 p. <https://doi.org/10.4095/289095>
- Hayes, B.J.R., 2011. Regional characterization of shale gas and shale oil potential, Northwest Territories; Northwest Territories Geoscience Office, NWT Open File 2011-08, 34 p.
- Hildred, G.V., Ratcliffe, K., and Schmidt, K. 2011. Application of inorganic whole-rock geochemistry to shale resource plays: an example from the Eagle Ford Shale, Texas; *Houston Geological Society, Bulletin*, p. 31–38.
- Hogg, J., 2015. The Canol oil shale play, central Mackenzie Valley, Northwest Territories, Canada: geoscience, operations and social license; Playmaker Conference, Canadian Society of Petroleum Geologists, Calgary. <<http://www.cspg.org/cspg/documents/Conference%20Website/Play%20Maker/Presentations/Hogg.pdf>> [accessed May 3, 2019]
- Hogue, B.C. and Gal, L.P., 2008. NWT formation tops for petroleum exploration and production wells: 60 to 80°N; Northwest Territories Geoscience Office, NWT Open File 2008-002.
- Hulbert, L.J., Carne, R., Gregoire, D., and Paktunc, D., 1992. Sedimentary nickel, zinc, and platinum-group-element mineralization in Devonian black shales at the Nick Property, Yukon, Canada: a new deposit type; *Exploration and Mining Geology*, v. 1, p. 39–62.
- Hume, G.S., 1954. Lower Mackenzie River area, Northwest Territories and Yukon; Geological Survey of Canada, Memoir 273, 118 p. <https://doi.org/10.4095/101498>
- Hume, G.S. and Link, T.A., 1945. Geological investigations in the Mackenzie River area, Northwest Territories; Geological Survey of Canada, Paper 45-16, 87 p. <https://doi.org/10.4095/101370>
- Hutchison, M.P. and Fraser, T.A., 2015. Palaeoenvironment, palaeohydrography and chemostratigraphic zonation of the Canol Formation, Richardson Mountains, north Yukon; in *Yukon exploration and geology 2014*, (ed.) K.E. MacFarlane and M.G. Nordling; Yukon Geological Survey, p. 73–98.
- Indigenous and Northern Affairs Canada, 2014. Exploration activities in the North; Chapter 3 in *Northern oils and gas annual report 2013*; Government of Canada, Indigenous and Northern Affairs Canada <<http://www.aadnc-aandc.gc.ca/eng/1398800136775/1398800252896#chp3>> [accessed March 30, 2020]
- Issler, D.R., Grist, A.M., and Stasiuk, L.D., 2005. Post-Early Devonian thermal constraints on hydrocarbon source rock maturation in the Keele tectonic zone, Tulita area, NWT, Canada, from multi-kinetic apatite fission track thermochronology, vitrinite reflectance and shale compaction; *Canadian Petroleum Geology Bulletin*, v. 53, p. 405–431. <https://doi.org/10.2113/53.4.405>
- Jackson, D.E. and Lenz, A.C., 1962. Zonation of Ordovician and Silurian graptolites in northern Yukon, Canada; *American Association of Petroleum Geologists, Bulletin*, v. 46, p. 30–45. <https://doi.org/10.1306/BC743757-16BE-11D7-8645000102C1865D>
- Jenkyns, H. C., 2010. Geochemistry of oceanic anoxic events; *Geochemistry, Geophysics, Geosystems*, v. 11, no. 3, 30 p. <https://doi.org/10.1029/2009GC002788>
- Jiang, C., Obermajer, M., Kabanov, P., and Mort, A., 2020. Organic geochemical data from northern Canada. Part II: Biomarkers in organic extracts from Devonian black shales (Horn River Group and basal Imperial Formation), Norman Wells area, Northwest Territories; Geological Survey of Canada, Open File 8663, 7 p. <https://doi.org/10.4095/321479>
- Joachimski, M.M., Pancost, R.D., Freeman, K.H., Ostertag-Henning, C., and Buggisch, W., 2002. Carbon isotope geochemistry of the Frasnian–Famennian transition; *Palaeogeography, Palaeoclimatology, Palaeoecology*, v. 181, p. 91–109. [https://doi.org/10.1016/S0031-0182\(01\)00474-6](https://doi.org/10.1016/S0031-0182(01)00474-6)
- Jones, A. L. and Gal, L.P., 2007. Northwest Territories oil and gas poster series: basins and petroleum resources, table of formations, schematic cross-sections; Northwest Territories Geoscience Office, NWT Open File 2007-003.
- Johnson, J.G., Klapper, G., and Sandberg, C.A., 1985. Devonian eustatic fluctuations in Euramerica; *Geological Society of America, Bulletin* 96, p. 567–587. [https://doi.org/10.1130/0016-7606\(1985\)96%3c567:DEFIE%3e2.0.CO;2](https://doi.org/10.1130/0016-7606(1985)96%3c567:DEFIE%3e2.0.CO;2)

- Kabanov, P.B., 2013. Revisiting legacy core and cross sections from the sub-Imperial Devonian of Mackenzie River corridor with emphasis on formation boundaries. Part 1: Wells Kugaluk N-02, Norman Wells P32X, Imperial Bear Island R34X, Maida Creek F57, and Devo Creek P45; Geological Survey of Canada, Open File 7466, 59 p. <https://doi.org/10.4095/292866>
- Kabanov, P.B., 2014. Landry Formation of Kugaluk N-02 well (Devonian, northern mainland NWT): insight into formation's boundaries, lithofacies, and stratal stacking patterns; Bulletin of Canadian Petroleum Geology, v. 62, p. 105–124. <https://doi.org/10.2113/gscpgbull.62.2.105>
- Kabanov, P.B., 2015. Geological and geochemical data from the Mackenzie region. Part I: Devonian cored sections and results for 2014 on geochemistry,  $\delta^{13}\text{C}$ – $\delta^{18}\text{C}$ , and Rock-Eval 6 pyrolysis; Geological Survey of Canada, Open File 7840, 90 p. <https://doi.org/10.4095/297403>
- Kabanov, P., 2017a. Stratigraphic unconformities: review of the concept and examples from the middle–upper Paleozoic; Chapter 6 in *Seismic and sequence stratigraphy and integrated stratigraphy — new insights and contributions*, (ed.) G. Aiello; InTechOpen, p. 101–127. <https://doi.org/10.5772/intechopen.70373>
- Kabanov, P., 2017b. Geological and geochemical data from Mackenzie Corridor. Part VII: New geochemical, Rock-Eval 6, and field data from the Ramparts and Canol formations of northern Mackenzie Valley, Northwest Territories; Geological Survey of Canada, Open File 8341, 19 p. <https://doi.org/10.4095/306299>
- Kabanov, P., 2018. Geological and geochemical data from the Canadian Arctic Islands. Part XV: Basal strata of Devonian clastic wedge on Banks Island and correlation with mainland Northwest Territories; Geological Survey of Canada, Open File 8354, 39 p. <https://doi.org/10.4095/306368>
- Kabanov, P., 2019. Devonian (c. 388–375 Ma) Horn River Group of Mackenzie Platform (NW Canada) is an open-shelf succession recording oceanic anoxic events; Journal of the Geological Society, v. 176, p. 29–45. <https://doi.org/10.1144/jgs2018-075>
- Kabanov, P. and Borrero Gomez, M.-L., 2019. Geological and geochemical data from Mackenzie Corridor. Part IX: Descriptions and associated measurements of cores from the Middle and Upper Devonian, Northwest Territories; Geological Survey of Canada, Open File 8558, 162 p. <https://doi.org/10.4095/314982>
- Kabanov, P. and Deblonde, C., 2019. Geological and geochemical data from Mackenzie corridor. Part VIII: Middle–Upper Devonian lithostratigraphy, formation tops, and isopach maps in NTS areas 96 and 106, Northwest Territories and Yukon; Geological Survey of Canada, Open File 8552, 37 p. <https://doi.org/10.4095/314785>
- Kabanov, P. and Gouwy, S., 2017. The Devonian Horn River Group and the basal Imperial Formation of the central Mackenzie Plain, N.W.T., Canada: multiproxy stratigraphic framework of a black shale basin; Canadian Journal of Earth Sciences, v. 54, p. 409–429. <https://doi.org/10.1139/cjes-2016-0096>
- Kabanov, P. and Jiang, C. 2020. Photic-zone euxinia and anoxic events in a Middle–Late Devonian shelfal sea of Panthalassan continental margin, NW Canada: changing paradigm of Devonian ocean and sea level fluctuations; Global and Planetary Change, v. 188. <https://doi.org/10.1016/j.gloplacha.2020.103153>
- Kabanov, P., Fallas, K.M., and Deblonde, C., 2016a. Geological and geochemical data from Mackenzie Corridor. Part IV: Formation tops and isopach maps of Horn River Group and basal beds of Imperial Formation, central Mackenzie Plain, NTS map sheets 96C–E; Geological Survey of Canada, Open File 8023, 14 p. <https://doi.org/10.4095/297903>
- Kabanov, P., Gouwy, S.A., and Chan, W.C., 2016b. Geological and geochemical data from Mackenzie Corridor. Part VI: Descriptions and SGR logs of Devonian outcrop sections, Mackenzie Mountains, Northwest Territories, NTS areas 106G and 106H; Geological Survey of Canada, Open File 8173, 93 p. <https://doi.org/10.4095/299434>
- Kabanov, P., Gouwy, S., Lawrence, P.W., Welischuk, D.J., and Chan, W.C., 2016c. Geological and geochemical data from Mackenzie Corridor. Part III: New data on lithofacies, micropaleontology, lithochem, and Rock-Eval™ pyrolysis from the Devonian Horn River Group in the Mackenzie Plain and Norman Range; Geological Survey of Canada, Open File 7951, 52 p. <https://doi.org/10.4095/297832>
- Kabanov, P., Percival, J.B., Bilot, I., and Jiang, C., 2016d. Geological and geochemical data from Mackenzie Corridor. Part V: New XRD data from Devonian cores and mineralogical characterization of mudrock units; Geological Survey of Canada, Open File 8168, 23 p. <https://doi.org/10.4095/299435>
- Kabanov, P., VandenBerg, R., Gouwy, S., van der Boon, A., Thallner, D., and Biggin, A., 2019. Geological and geochemical data from Mackenzie Corridor. Part X: Reference sections of Middle–Upper Devonian strata at Prohibition Creek, Norman Range, Northwest Territories; Geological Survey of Canada, Open File 8648, 36 p. <https://doi.org/10.4095/321379>
- Kabanov, P., Vandenberg, R., Pelchat, P., Cameron, M., and Dewing, K., 2020. Lithostratigraphy of Devonian basinal mudrocks in frontier areas of northwestern Canada augmented with ED-XRF technique; arktos, v. 6, p. 39–52. <https://doi.org/10.1007/s41063-020-00074-z>
- Kaiser, S.I., Aretz, M., and Becker, R.T., 2015. The global Hangenberg crisis (Devonian–Carboniferous transition): review of a first-order mass extinction; Geological Society of London, Special Publications, v. 423, p. 387–437. <https://doi.org/10.1144/SP423.9>
- Kidder, D.L. and Worsley, T.R., 2010. Phanerozoic large igneous provinces (LIPs), HEATT (haline euxinic acidic thermal transgression) episodes, and mass extinctions; Palaeogeography, Palaeoclimatology, Palaeoecology, v. 295, p. 162–191. <https://doi.org/10.1016/j.palaeo.2010.05.036>
- Kindle, E.M. and Bosworth, T.O., 1921. Oil-bearing rocks of lower Mackenzie River valley; Geological Survey of Canada, Summary Report, Part B, p. 37–63. <https://doi.org/10.4095/103621>
- Kravchinsky, V.A., 2012. Paleozoic large igneous provinces of northern Eurasia: correlation with mass extinction events; Global and Planetary Change, v. 86–87, p. 31–36. <https://doi.org/10.1016/j.gloplacha.2012.01.007>

- Lane, L.S., 2007. Devonian–Carboniferous paleogeography and orogenesis, northern Yukon and adjacent Arctic Alaska; *Canadian Journal of Earth Sciences*, v. 44, p. 679–694. <https://doi.org/10.1139/e06-131>
- Law, J., 1971. Regional Devonian geology and oil and gas possibilities, upper Mackenzie River area; *Bulletin of Canadian Petroleum Geology*, v. 19, p. 437–486.
- Lenz, A.C. and Pedder, A.E.H., 1972. Lower and middle Paleozoic sediments and paleontology of Royal Creek and Peel River, Yukon, and Powell Creek, N.W.T.; XXIV International Geological Congress, Field excursion guidebook, v. A14, 43 p.
- Lemieux, Y., Hadlari, T., and Simonetti, A., 2011. Detrital zircon geochronology and provenance of Devonian–Mississippian strata in the northern Canadian Cordilleran miogeocline; *Canadian Journal of Earth Sciences*, v. 48, p. 515–541. <https://doi.org/10.1139/E10-056>
- MacKenzie, W.S., 1970. Allochthonous reef-debris – limestone turbidites, Powell Creek, Northwest Territories; *Bulletin of Canadian Petroleum Geology*, v. 18, p. 474–492.
- MacKenzie, W.S., 1973. Upper Devonian echinoderm debris beds with graded texture, District of Mackenzie, Northwest Territories; *Canadian Journal of Earth Sciences*, v. 10, p. 519–528. <https://doi.org/10.1139/e73-051>
- MacKenzie, W.S., 1974. Lower Paleozoic carbonates, C.D.R. Tenlen Lake A-73 well, Northwest Territories; in *Report of activities, Part B*; Geological Survey of Canada, Paper 74-1B, p. 265–270. <https://doi.org/10.4095/104771>
- MacLean, B.C., 2011. Tectonic and stratigraphic evolution of the Cambrian basin of the northern Northwest Territories; *Bulletin of Canadian Petroleum Geology*, v. 59, p. 172–194. <https://doi.org/10.2113/gscpgbull.59.2.172>
- MacLean, B.C., 2012. GIS-enabled structure maps of subsurface Phanerozoic strata, northwestern Northwest Territories; Geological Survey of Canada, Open File 7172, zip file. <https://doi.org/10.4095/292152>
- MacLean, B.C., Fallas, K.M., and Hadlari, T., 2015. The evolution of Keele Arch, a multiphase feature of the northern mainland, Northwest Territories; Geological Survey of Canada, Bulletin 606, 47 p. <https://doi.org/10.4095/293877>
- Meijer Drees, N.C., 1993. The Devonian succession in the subsurface of the Great Slave and Great Bear Plains, Northwest Territories; Geological Survey of Canada, Bulletin 393, 231 p. <https://doi.org/10.4095/183905>
- Meyer, K.M. and Kump, L.R., 2008. Oceanic euxinia in Earth history: causes and consequences; *Annual Review of Earth and Planetary Sciences*, v. 36, p. 251–288. <https://doi.org/10.1146/annurev.earth.36.031207.124256>
- Morrow, D.W., 1982. Descriptive field classification of sedimentary and diagenetic breccia fabrics in carbonate rocks; *Bulletin of Canadian Petroleum Geology*, v. 30, p. 227–229.
- Morrow, D.W., 1991. The Silurian–Devonian sequence of the northern part of the Mackenzie Shelf, Northwest Territories; Geological Survey of Canada, Bulletin 413, 128 p. <https://doi.org/10.4095/132170>
- Morrow, D.W., 1999. Lower Paleozoic stratigraphy of northern Yukon Territory and northwestern district of Mackenzie; Geological Survey of Canada, Bulletin 538, 202 p. <https://doi.org/10.4095/210998>
- Morrow, D.W., 2012. Devonian of the northern Canadian Mainland Sedimentary Basin (a contribution to the Geological atlas of the northern Canadian Mainland Sedimentary Basin); Geological Survey of Canada, Open File 6997, 88 p. <https://doi.org/10.4095/290970>
- Morrow, D.W., 2018. Devonian of the northern Canadian Mainland Sedimentary Basin: a review; *Bulletin of Canadian Petroleum Geology*, v. 66, p. 623–694.
- Morrow, D.W. and Cook, D.G., 1987. The Prairie Creek embayment and lower Paleozoic stratigraphy of the southern Mackenzie Mountains; Geological Survey of Canada, Memoir 412, 195 p. <https://doi.org/10.4095/122458>
- Morrow, D.W. and Geldsetzer, H.H.J., 1988. Devonian of the eastern Canadian Cordillera; in *Devonian of the world, Proceedings of the Second International Symposium on the Devonian System, Volume I, Regional syntheses*, (ed.) N.J. McMillan, A.F. Embry, and D.J. Glass; Canadian Society of Petroleum Geologists, Memoir 14, p. 85–121.
- Morrow, D.W. and Meijer Drees, N.C., 1981. The Early to Middle Devonian Bear Rock Formation in the type section and in other surface sections, District of Mackenzie; in *Current research, Part A*; Geological Survey of Canada, Paper 81-1A, p. 107–114. <https://doi.org/10.4095/109640>
- Muir, I.D., 1988. Devonian Hare Indian and Ramparts formations, Mackenzie Mountains, N.W.T.: basin-fill, platform and reef development; Ph.D. thesis, University of Ontario, Ottawa, Ontario, 661 p. <https://doi.org/10.20381/ruor-10585>
- Muir, I. and Dixon, O.A., 1985. Devonian Hare Indian–Ramparts evolution, Mackenzie Mountains, NWT, basin-fill and platform-reef development; in *Contributions to the geology of the Northwest Territories, Volume 2*, (ed.) J.A. Brophy; Department of Indian and Northern Affairs, p. 85–90.
- Muir, I., Wong, P., and Wendte, J., 1984. Devonian Hare Indian–Ramparts (Kee Scarp) evolution, Mackenzie Mountains and subsurface Norman Wells, N.W.T.: basin-fill and platform development; in *Carbonates in subsurface and outcrop*, (ed.) L. Eliuk, J. Kaldi, and N. Watts; Canadian Society of Petroleum Geologists Core Conference, Calgary, Alberta, October 18–19, 1984, p. 82–102.
- Narkiewicz, K. and Bultynck, P., 2007. Conodont biostratigraphy of shallow marine Givetian deposits from the Radom–Lublin area (SE Poland); *Geological Quarterly*, v. 51, p. 419–442.
- National Energy Board – Northwest Territories Geological Survey, 2015. Energy briefing note: an assessment of the unconventional petroleum resources of the Bluefish Shale and the Canol Shale in the Northwest Territories; National Energy Board and Northwest Territories Geological Survey, 10 p. <<https://www.neb-one.gc.ca/nrg/sttsc/crdlndptlmpdct/rprt/2015shlnt/index-eng.html>> [accessed January 29, 2021]
- Norford, B.S. and Macqueen, R.W., 1975. Lower Paleozoic Franklin Mountain and Mount Kindle formations, District of Mackenzie: their type sections and regional development; Geological Survey of Canada, Paper 74-34, 45 p. <https://doi.org/10.4095/102525>



- Norris, A.W., 1968. Reconnaissance Devonian stratigraphy of northern Yukon Territory and northwestern District of Mackenzie; Geological Survey of Canada, Paper 67-53, 287 p. <https://doi.org/10.4095/101441>
- Norris, A.W., 1985. Stratigraphy of Devonian outcrop belts in northern Yukon Territory and Northwest Territories, District of Mackenzie (Operation Porcupine area); Geological Survey of Canada, Memoir 410, 81 p. <https://doi.org/10.4095/120309>
- Norris, A.W., 1997. Devonian; Chapter 7 in *Geology and mineral and hydrocarbon potential of northern Yukon Territory and northwestern District of Mackenzie*, (ed.) D.K. Norris; Geological Survey of Canada, Bulletin 422, p. 163–200. <https://doi.org/10.4095/208893>
- Norris, D.K., 1981. *Geology, Eagle River, Yukon Territory*; Geological Survey of Canada, Map 1523A, scale 1:250 000. <https://doi.org/10.4095/109352>
- North American Commission on Stratigraphic Nomenclature, 2005. North American Stratigraphic Code; American Association of Petroleum Geologists, Bulletin, v. 89, p. 1547–1591. <https://doi.org/10.1306/07050504129>
- Ootes, L., Gleeson, S.A., Turner, E.T., Rasmussen, K., Gordey, S., Falck, H., Martel, E., and Pierce, K., 2013. Metallogenic evolution of the Mackenzie and eastern Selwyn mountains of Canada's northern Cordillera, Northwest Territories: a compilation and review; *Geoscience Canada*, v. 40, p. 40–69. <https://doi.org/10.12789/geocanj.2013.40.005>
- Peters, K.E. and Cassa, M.R., 1994. Applied source rock geochemistry; in *The petroleum system — from source to trap*, (ed.) L.B. Magoon and W.G. Dow; American Association of Petroleum Geologists, Memoir 60, p. 93–117. <https://doi.org/10.1306/M60585C5>
- Pope, M.C. and Leslie, S.A., 2013. New data from Late Ordovician–early Silurian Mount Kindle Formation measured sections, Franklin Mountains and eastern Mackenzie Mountains, Northwest Territories; Geological Survey of Canada, Current Research 2013-8, 14 p. <https://doi.org/10.4095/292389>
- Powell, J., 2017. Burial and exhumation history of the Mackenzie Mountains and Plain, NWT, through integration of low-temperature thermochronometers; Ph.D. thesis, University of Ottawa, Ottawa, Ontario, 363 p. <https://doi.org/10.20381/ruor-20274>
- Powell, J., Schneider, D., Stockli, D., and Fallas, K., 2016. Zircon (U-Th)/He thermochronology of Neoproterozoic strata from the Mackenzie Mountains, Canada: implications for the Phanerozoic exhumation and deformation history of the northern Canadian Cordillera; *Tectonics*, v. 35, p. 663–689. <https://doi.org/10.1002/2015TC003989>
- Pugh, D.C., 1983. Pre-Mesozoic geology in the subsurface of Peel River map area, Yukon Territory and District of Mackenzie; Geological Survey of Canada, Memoir 401, 61 p. <https://doi.org/10.4095/119498>
- Pugh, D.C., 1993. Subsurface geology and pre-Mesozoic strata, Great Bear River map area, District of Mackenzie; Geological Survey of Canada, Memoir 430, 137 p. <https://doi.org/10.4095/183985>
- Pyle, L.J. and Gal, L.P., 2009. Cambrian–Ordovician to Silurian strata and lower Paleozoic (Ronning Group) platform play; Chapter 4 in *Regional geoscience studies and petroleum potential, Peel Plateau and Plain, Northwest Territories and Yukon, Project Volume*, (ed.) L.J. Pyle and A.L. Jones; Northwest Territories Geoscience Office and Yukon Geological Survey, NWT Open File 2009-02 and YGS Open File 2009-25, p. 112–160.
- Pyle, L.J. and Gal, L.P., 2012. Measured sections and petroleum potential data (conventional and unconventional) of Horn River Group outcrops, NTS 95M, 95N, 96C, 96D, 96E, 106H, and 106I, Northwest Territories — Part II; Northwest Territories Geoscience Office, N.W.T. Open File Report 2012-008, 114 p.
- Pyle, L.J. and Gal, L.P., 2013. Measured sections and petroleum potential data (conventional and unconventional) of Horn River Group outcrops, NTS 96C, 96E, and 106H, Northwest Territories — Part III; Northwest Territories Geoscience Office, N.W.T. Open File Report 2013-005, 73 p.
- Pyle, L.J. and Gal, L.P., 2016. Reference section for the Horn River Group and definition of the Bell Creek Member, Hare Indian Formation in central Northwest Territories; *Bulletin of Canadian Petroleum Geology*, v. 64, p. 67–98. <https://doi.org/10.2113/gscpgbull.64.1.67>
- Pyle, L.J. and Jones, A.L., 2009. Introduction; Chapter 1 in *Regional geoscience studies and petroleum potential, Peel Plateau and Plain, Northwest Territories and Yukon, Project Volume*, (ed.) L.J. Pyle and A.L. Jones; Northwest Territories Geoscience Office and Yukon Geological Survey, NWT Open File 2009-02 and YGS Open File 2009-25, p. 1–42.
- Pyle, L.J., Gal, L.P., and Fiess, K.M., 2014. Devonian Horn River Group: a reference section, lithogeochemical characterization, correlation of measured sections and wells, and petroleum-potential data, Mackenzie Plain area (NTS 95M, 95N, 96C, 96D, 96E, 106H, and 106I), NWT; Northwest Territories Geoscience Office, NWT Open File Report 2014-06, 70 p.
- Pyle, L.J., Gal, L.P., and Hadlari, T., 2015. Thermal maturity trends for Devonian Horn River Group units and equivalent strata in the Mackenzie Corridor, Northwest Territories and Yukon; Geological Survey of Canada, Open File 7850, 44 p. <https://doi.org/10.4095/296446>
- Racki, G., 2020. A volcanic scenario for the Frasnian–Famennian major biotic crisis and other Late Devonian global changes: more answers than questions?; *Global and Planetary Change*, v. 189, art. 103174, 29 p. <https://doi.org/10.1016/j.gloplacha.2020.103174>
- Richards, B.C., 1989. Upper Kaskaskia Sequence: uppermost Devonian and lower Carboniferous; Chapter 9 in *Western Canada Sedimentary Basin, a case history*, (ed.) B.D. Ricketts; Canadian Society of Petroleum Geologists, Special Publication 30, p. 165–201.
- Richards, B.C., Ross, G.M., and Utting, J., 2002. U-Pb geochronology, lithostratigraphy and biostratigraphy of tuff in the upper Famennian to Tournaisian Exshaw Formation: evidence for a mid-Paleozoic magmatic arc on the northwestern margin of North America; in *Carboniferous and Permian of the world*, (ed.) L.V. Hills, C.M. Henderson, and E.W. Bamber; Canadian Society of Petroleum Geologists, Memoir 19, p. 158–207.

- Rocheleau, J. and Fiess, K.M., 2014. Northwest Territories oil and gas poster series: basins and petroleum resources, table of formations, schematic cross sections; Northwest Territories Geoscience Office, NWT Open File Report 2014-03, 3 posters.
- Sandberg, C.A., Morrow, J.R., and Ziegler, W., 2002. Late Devonian sea-level changes, catastrophic events, and mass extinctions; *in* Catastrophic events and mass extinctions: impacts and beyond, (ed.) C. Koeberland K.G. MacLeod; Geological Society of America, GSA Special Papers, v. 356, p. 473–487. <https://doi.org/10.1130/SPE356>
- Schlager, W., 1989. Drowning unconformities on carbonate platforms; *in* Controls on carbonate platform and basin development, (ed.) P.D. Crevello, J.L. Wilson, J.F. Sarg, and J.F. Read; Society for Sedimentary Geology, SEPM Special Publication 41, p. 15–25. <https://doi.org/10.2110/pec.89.44.0015>
- Schlager, W. 2005. Carbonate sedimentology and sequence stratigraphy; Society for Sedimentary Geology, SEPM Concepts in Sedimentology and Paleontology, v. 8, 200 p. <https://doi.org/10.2110/csp.05.08>
- Sloss, L.L., 1963. Sequences in the cratonic interior of North America; Geological Society of America, Bulletin, v. 74, p. 93–113.
- Snowdon, L.R., Brooks, P.W., Williams, G.K., and Goodarzi, F., 1987. Correlation of the Canol Formation source rock with oil from Norman Wells; Organic Geochemistry, v. 11, p. 529–548. [https://doi.org/10.1016/0146-6380\(87\)90008-8](https://doi.org/10.1016/0146-6380(87)90008-8)
- Strauss, J.V., Fraser, T., Melchin, M.J., Allen, T.J., Malinowski, J., Feng, X., Taylor, J.F., Day, J., Gill, B.C., and Sperling, E.A., 2020. The Road River Group of northern Yukon, Canada: early Paleozoic deep-water sedimentation within the Great American Carbonate Bank; Canadian Journal of Earth Sciences, v. 57, p. 1193–1219. <https://doi.org/10.1139/cjes-2020-0017>
- Tassonyi, E.J., 1969. Subsurface geology, lower Mackenzie River and Anderson River area, district of Mackenzie; Geological Survey of Canada, Paper 68-25, 207 p. <https://doi.org/10.4095/103335>
- Taylor, A.M. and Goldring, R., 1993. Description and analysis of bioturbation and ichnofabric; Journal of the Geological Society, v. 150, p. 141–148. <https://doi.org/10.1144/gsjgs.150.1.0141>
- Taylor, A.M., Goldring, R., and Gowland, S., 2003. Analysis and application of ichnofabrics; Earth-Science Reviews, v. 60, p. 227–259. [https://doi.org/10.1016/S0012-8252\(02\)00105-8](https://doi.org/10.1016/S0012-8252(02)00105-8)
- Vopni, L.K. and Lerbekmo, J.F., 1972. Sedimentology and ecology of the Horn Plateau Formation: a Middle Devonian coral reef, Northwest Territories, Canada; Geologische Rundschau, v. 61, p. 626–646. <https://doi.org/10.1007/BF01896338>
- Whittaker, E.J., 1922. Mackenzie River district between Great Slave Lake and Simpson; Geological Survey of Canada, Summary Report, 1921, Part B, p. 45–55. <https://doi.org/10.4095/293541>
- Williams, G.K., 1975. “Arnica platform dolomite” (NTS 85, 95, 96, 105, 106), district of Mackenzie; *in* Report of activities, Part C; Geological Survey of Canada, Paper 75-1C, p. 31–35. <https://doi.org/10.4095/103021>
- Williams, G.K., 1983. What does the term ‘Horn River’ mean? A review; Bulletin of Canadian Petroleum Geology, v. 31, p. 117–122.
- Williams, G.K., 1989. Tectonic evolution of the Fort Norman area, Mackenzie Corridor, N.W.T.; Geological Survey of Canada, Open File 2045, 98 p. <https://doi.org/10.4095/130647>
- Williams, G.K., 1996. Stratigraphy and tectonics of the Ronning and Delorme Groups, Northwest Territories; Geological Survey of Canada, Open File 3212, 81 p. <https://doi.org/10.4095/205762>
- Williams, M.Y., 1922. Exploration east of Mackenzie River between Simpson and Wrigley; Geological Survey of Canada, Summary Report, 1921, Part B, p. 56–66. <https://doi.org/10.4095/293541>
- Wohlberg, M., 2014. MGM shut-down opens up N.W.T. oil leases; *Northern Journal*, April 2014, <<http://norj.ca/2014/04/mgm-shut-down-opens-up-nwt-oil-leases>> [accessed April 03, 2020]
- Yose, L.A., Brown, S., Davis, T.L., Eiben, T., Kompanik, G.S., and Maxwell, S.R., 2001. 3-D geologic model of a fractured carbonate reservoir, Norman Wells Field, NWT, Canada; Bulletin of Canadian Petroleum Geology, v. 49, p. 86–116. <https://doi.org/10.2113/49.1.86>